Pulsed Gradient Spin−Echo (PGSE) Diffusion and ¹H,¹⁹F Heteronuclear Overhauser Spectroscopy (HOESY) NMR Methods in Inorganic and Organometallic Chemistry: Something Old and Something New

Paul S. Pregosin,* P. G. Anil Kumar, and Ignacio Fernández

Laboratory of Inorganic Chemistry, ETHZ, Hönggerberg, CH-8093 Zürich, Switzerland

Contents

1. Methodology

The determination of relative molecular size in solution remains a subject of considerable interest to the chemistry community. This is especially true with respect to the formation of polymers, biopolymers, polynuclear materials, and otherwise aggregated materials. Apart from mass spectroscopic methods, diffusion methods have found increasing favor in this area.

Pulsed gradient spin−echo (PGSE) NMR diffusion methods were introduced ca. 40 years ago by Stejskal and Tanner[1] and represent a possible supplement to mass spectroscopy. The basic NMR experiment is based on a spin−echo sequence and two incorporated pulsed field gradients separated by a waiting time, Δ (see Figure 1). The effect of the two gradients is to

Figure 1. Typical pulse sequences for the PGSE experiments: (a) the Stejskal−Tanner experiment; (b) the Stejskal−Tanner experiment modified via substitution of two 90° pulses for a single 180° pulse.

initially defocus and then refocus the magnetization; however, if during the time Δ the molecules diffuse from their positions after the first gradient pulse, the effective magnetic field experienced by the spins will be different during both gradient pulses. This results in incomplete refocusing of the spins and a consequent decrease in the intensity of the resulting NMR signals. Repetition of the experiment with increasing gradient strengths, *G*, affords a set of signals from which the diffusion coefficient, *D* (often called a "self-diffusion constant", in the literature), can be obtained (see eq 1).

$$\ln(I/I_0) = -\gamma_X^2 \delta^2 G^2 (\Delta - \delta/3) D \qquad (1)$$

γ_X = gyromagnetic ratio of the X nucleus;
δ = length of the gradient pulse;   *G* = gradient strength;
Δ = delay between the midpoints of the gradients;
D = diffusion coefficient

A typical plot of the observed intensity changes, $\ln(I/I_0)$, as a function G^2 is shown in Figure 2. Molecules (or ions) possessing larger volumes will diffuse more slowly than smaller molecules and thus afford smaller slopes.

More elaborate pulse sequences[2] have been proposed and the stimulated spin−echo[2a] (see Figure 1b), in which three 90° pulses are used, has the advantage that the signals decay according to T_1 (spin−lattice relaxation time) rather than according to T_2 (spin−spin relaxation time).

Given that the PGSE methodology stems from the relatively early days of NMR, a substantial body of literature exists, and the subject has been reviewed on several occasions.[3,4] The diffusion literature includes applications from the fields of biology and medicine,[5−8] polymers,[9−11] colloids,[12] and organic,[13−18] inorganic,[19−26] and physical chemistry/spectroscopy.[27−34] The references cited are mostly from the recent literature.

PGSE data may also be presented as one component of a 2D spectrum in which the chemical shift is displayed in the first dimension and the diffusion coefficient in the second one. Such an experiment is called DOSY (diffusion ordered spectroscopy, see Figure 3)[35−39] and has also been referred to as "NMR chromatography", for its ability to facilitate and visualize the resolution and assignment of complex
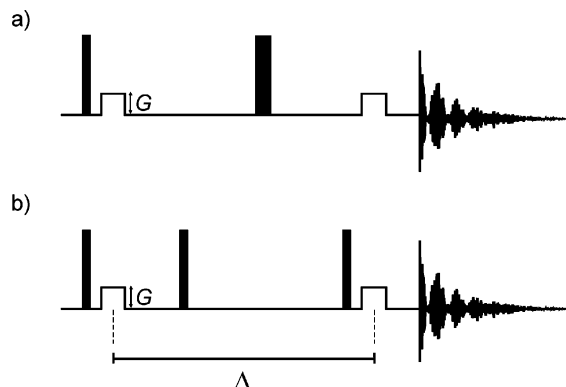
Paul Pregosin was born in New York City in 1943 and received his Ph.D. from the City University of New York in 1970. After postdoctoral studies at Queen Mary College in London, U.K., and the University of Delaware in Newark, he moved to the ETHZ in 1973 where he has remained ever since. His research interests include organometallic chemistry, homogeneous catalysis, and NMR spectroscopy.
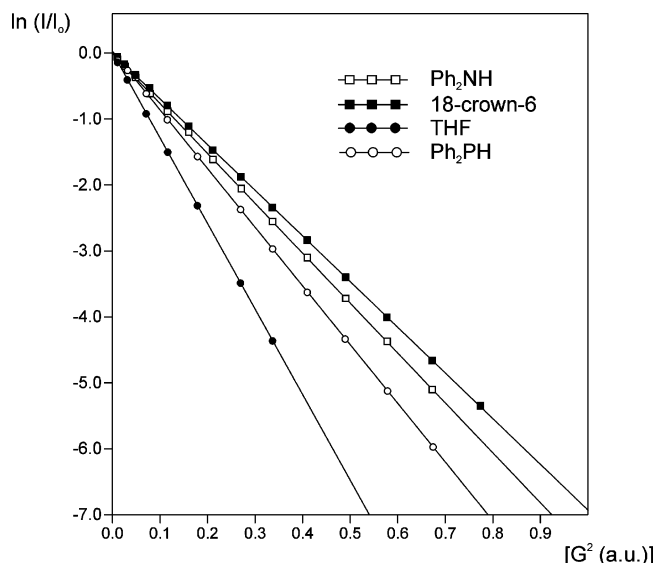

Anil Kumar P. G. was born in Chickmagalur, India, in 1977. He graduated in Inorganic Chemistry from Bangalore University in 1999. He has just finished his Ph.D. (March 2005) under the supervision of Prof. Pregosin at ETHZ, Switzerland. His thesis focused on "PGSE Diffusion and Multidimensional NMR Studies on Late Transition Metal Complexes: Applications in Homogeneous Catalysis".


Ignacio Fernández was born in Spain in 1976 and obtained his Ph.D. from the University of Almería in 2003. He has been involved in several student exchange programs, which took him first to Bath (2000) with Prof. Matthew G. Davidson, to Würzburg with Prof. Dietmar Stalke (2001), and then to Zürich (2003). He is currently working as a postdoctoral fellow in the research group of Prof. P. S. Pregosin at the ETHZ. His current research interests are focused on the applications of multinuclear NMR studies to problems in organometallic chemistry.

Figure 2. Typical plot of the observed intensity changes, $\ln(I/I_0)$, as a function of G^2 showing various translation rates depending on their molecular sizes for various species (see inset) in solution. The data stem from four different measurements (I. Fernández, unpublished results, ETHZ, 2004).
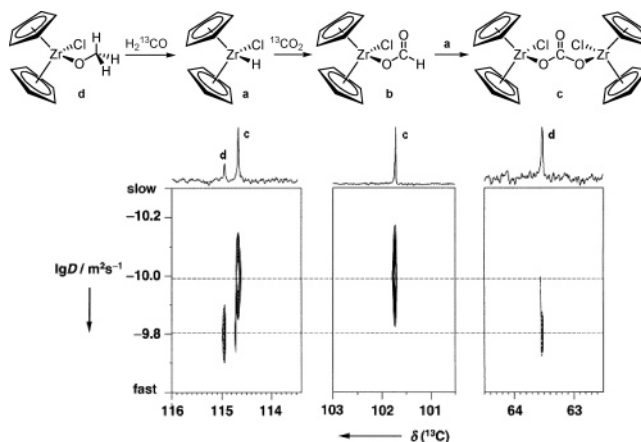
Figure 3. ^{13}C INEPT DOSY spectrum[22a] obtained during the reaction of **a** with $^{13}CO_2$ at -78 °C in THF-d_8. The sections show the signals of **c** ($\delta = 114.6$, Cp) and **d** ($\delta = 114.9$, Cp).

mixtures. DOSY methods (and a variety of pulse sequences are now commonly in use[38b]) have proven especially valuable[40−48] where the molecules are relatively large and thus the NMR spectra are fairly complicated. Although the DOSY methodology is potentially quantitative, integrating cross-peaks is not always straightforward. The PGSE approach routinely gives diffusion constants that are accurate to $\pm 2\%$.

Generally, the PGSE methodology presents several advantages: it is fairly rapid for ^1H and ^{19}F (ca. $1−2$ h) and noninvasive and requires only small quantities of material (usually $1−2$ mM solutions) depending on the nucleus chosen. Several components of a mixture can be measured simultaneously (as long as they afford resolvable NMR signals), which makes the technique especially valuable for materials that are not readily isolable or for solutions containing a number of compounds, for example, a mixture of diastereomeric compounds or complexes or perhaps several species in equilibrium.

From the diffusion coefficients, it is possible to obtain the so-called hydrodynamic radius, r_H, via the Stokes−Einstein equation (see eq 2), which, in turn,

$$r_H = \frac{kT}{6\pi\eta D} \qquad (2)$$

allows one to estimate the molecular volume. Although this equation has its drawbacks[49,50] it is widely used when comparing D-values involving data from differing solvents because it provides a correction for solvent viscosity, η. The published correlations of r_H with radii from crystallography are reasonable,[51] and Figure 4 shows a typical correlation.
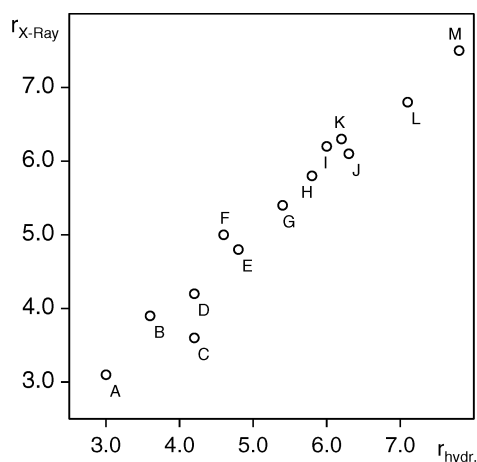

	Compound	r_H	r_{X-ray}
A	$ZrCl_2(Cp)_2$	3.0	3.1
B	$(Cp_2ZrCl)_2(\mu\text{-}O)$	3.7	3.9
C	$ZrCl(OMe)(Cp)_2$	4.2	3.6
D	$PdCl_2(AsMe_3)_2$	4.2	4.1
E	$PdCl_2(AsMe_2Ph)_2$	4.8	4.8
F	$Tp^{Me2}W(CO)_3H$	4.6	5.0
G	$PdCl_2(AsMePh_2)_2$	5.4	5.4
H	$PdCl_2(AsPh_3)_2$	5.8	5.8
I	$PdBr(C_6H_5)(MeOBiphep)$	6.0	6.2
J	$(Cp_2ZrCl)_2(\mu\text{-}O_2CH_2)$	6.3	6.1
K	$Pd_2(dba)_3$	6.2	6.3
L	$PdBr(C_6H_5CN)(Binap)$	7.1	6.8
M	$[Ru_2(\mu\text{-}Cl_3)(mesetph)_2]Cl$	7.8	7.5

Figure 4. Plot of hydrodynamic radii obtained from PGSE experiments vs the radii calculated from crystallographic data.[51] For compounds **D**, **E**, **G**, and **H**, the radii in the solid state were estimated using reported structures for analogous phosphine, instead of arsine. For **C** and **J**, the values were calculated from minimized gas-phase structures (PM3).

The trend in recent times is toward multinuclear PGSE studies. Apart from the high receptivity nuclei, ¹H and ¹⁹F,[17,26,28] PGSE diffusion measurements have been reported for ¹³C (see Figure 3[22]), ²⁹Si (in silicates),[39] ³¹P (for tertiary phosphine donors and their complexes[52–55]), ³⁵Cl (in perchlorate salts[52]), ⁷Li,[9,10,23,35,53] and most recently, ¹⁹⁵Pt (in the $PtCl_6^{2-}$ anion[54]) and ²³Na.[56] Figure 5 shows data from a ¹⁹F diffusion study using three fluorine-containing anions.[57]

For a routine PGSE measurement, there are by and large no major instrumental or sample requirements (apart from a spectrometer equipped with gradients), and 1−2 mM solutions are readily measured; however, problems can arise during variable
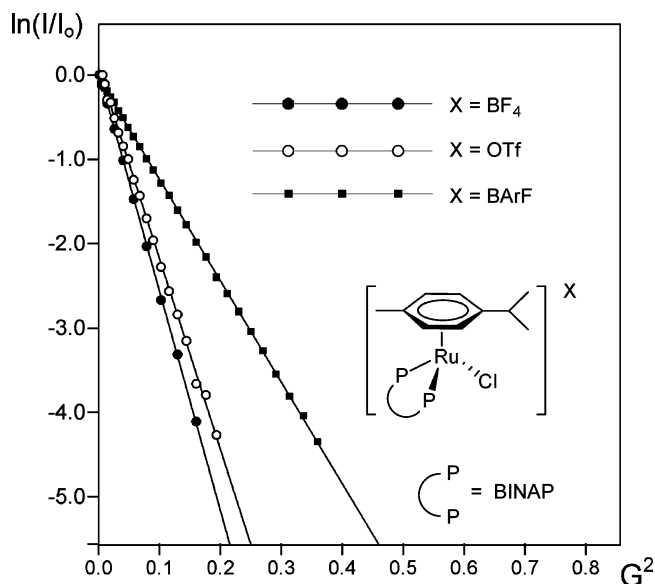
Figure 5. Plots of ¹⁹F $\ln(I/I_0)$ vs arbitrary units proportional to the square of the gradient amplitude on several salts of the cationic Ru(II) p-cymene BINAP complex shown. The larger the anion is, the smaller the absolute value of the slope becomes.[57]

temperature studies. Although one does not routinely spin the sample, convection can be a problem.[30,31,58,59] Convection currents are caused by small temperature gradients within the sample, which are difficult to eliminate. The general diffusion curve for a sample showing convection is illustrated in Figure 6.
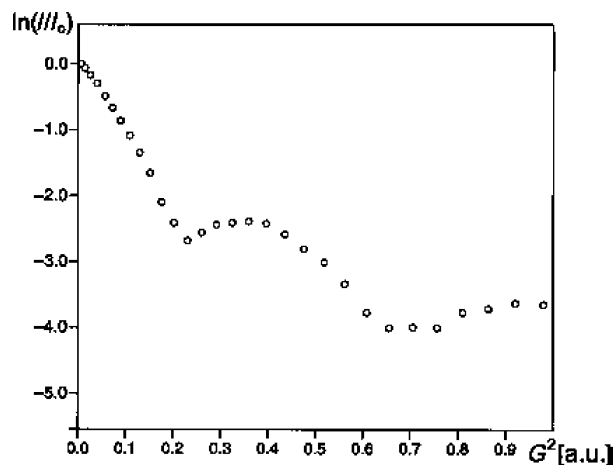
Figure 6. Plots of $\ln(I/I_0)$ vs arbitrary units proportional to the square of the gradient amplitude for several ¹H PGSE diffusion measurements at 228 K in a 5 mm NMR tube.[58]

Our solution[58] to the convection problem involved the use of a coaxial insert inside a normal 5 mm NMR tube (although different approaches have been recommended.[60,61] The inner and outer tubes are separated by a Pyrex spacer suitable for variable temperature experiments. A space of ca. 2 mm is left between both tubes at the bottom. Using this configuration, it is possible to obtain correct diffusion constants and temperature-independent hydrodynamic radii.

A sensitive test[58] for the onset of convection involves a comparison of D-values measured with

Table 1. ^{1}H and ^{19}F Diffusion Results[58] (10^{-10} m^2 s^{-1}) for 1 and 2 in CD$_2$Cl$_2$ at 231 K^{a,b} as a Function of Δ

nucleus	Δ (ms)	D^c	r_H (Å)	D	r_H (Å)
		1		**2**	
^{1}H	118	3.88(6), 3.87(6)	4.7(1)	2.83(6)	6.4(1)
	168	3.91(6), 3.90(6)	4.6(1)		
	268	3.93(6), 3.95(6)	4.6(1)	2.77(6)	6.5(1)
^{19}F	118	3.87(6), 3.84(6)	4.7(1)	3.72(6)	4.9(1)
	168	3.84(6), 3.89(6)	4.7(1)		
	268	3.95(6), 3.94(6)	4.6(1)	3.79(6)	4.8(1)

^{a} Both compounds in 10 mM concentration. ^{b} η(CH$_2$Cl$_2$) = 0.933 kg s^{-1} m^{-1}. ^{c} The results of two different samples prepared under similar conditions are shown.

different diffusion delays, Δ, because convection shows up as a Δ-dependent (apparent) diffusion coefficient. Table 1 shows diffusion data for two complexes, **1** and **2**, at 231 K as a function of the

1   **2**
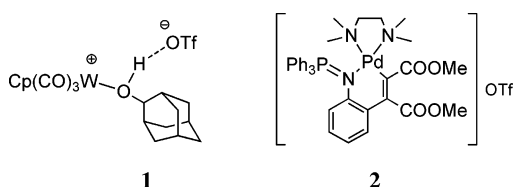
delay, Δ. Clearly, the coaxial insert approach seems to work well, because the data are quite reproducible; however, we note that, in some cases,[62-64] convection at low temperature does not seem to be a problem.

There are a number of possible reasons (aggregation, solvation, ion-pairing, etc.) why an r_H value, as calculated from the Stokes−Einstein equation, might not reflect the solid-state structure. However, clearly, temperature effects on solvent viscosity are important; consequently, it is often useful to use a small quantity of a reference compound. The two most often used are tetramethylsilane[65] and tetrakis-trimethylsilyl-silane, Si(SiMe$_3$)$_4$ (TMSS).[66] Assuming that the room-temperature D and r_H values of these approximately spherical molecules are well-known, one can estimate the solution viscosity at low temperature via the measured D-value of the reference together with eq 2.
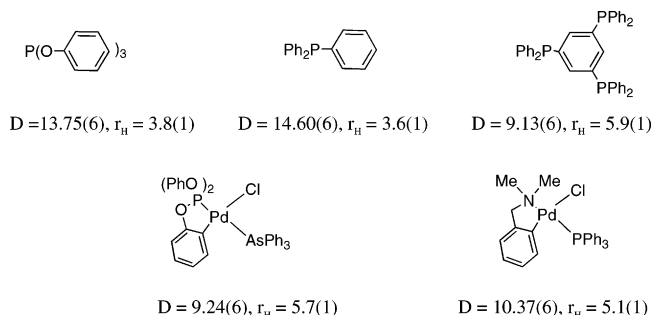
As an example, we note that there are no literature viscosity data for THF at 155 K, which is slightly below its freezing point. This temperature is sometimes needed for the measurement of materials that are dynamic on the NMR time scale. We have recently obtained[53] ^{1}H, ^{31}P, and ^{7}Li PGSE data for a 60 mM THF solution of LiPPh$_2$ at 155 K. A sample of TMSS of the same concentration and temperature was also measured. Since the r_H-value for TMSS at ambient temperature can be determined, the measured D-values at 155 K, together with the Stokes−Einstein equation,[53] afford a realistic estimate of the THF viscosity, η (10.4 × 10^{-3} kg s^{-1} m^{-1}), at 155 K.

2. Applications

2.1. Molecular Volumes

The most common PGSE application involves determining the relative volume of a compound via r_H

from the Stokes−Einstein equation. As the molecules become larger, they generally move slower (see Scheme 1). The more phenyl groups one has in the molecule, the slower will be the observed translation.

Scheme 1. ^{1}H Diffusion (D, 10^{-10} m^2 s^{-1}) and r_H (Å) Data in CD$_2$Cl$_2$ (10 mM)

D = 13.75(6), r_H = 3.8(1) D = 14.60(6), r_H = 3.6(1) D = 9.13(6), r_H = 5.9(1)

D = 9.24(6), r_H = 5.7(1) D = 10.37(6), r_H = 5.1(1)

A common application of PGSE methods in coordination chemistry concerns the recognition of a monomer−dimer equilibrium, the assignment of a di- (or poly-) nuclear rather than a mononuclear structure, or both. The gallium cluster, **3**, which in THF-


3
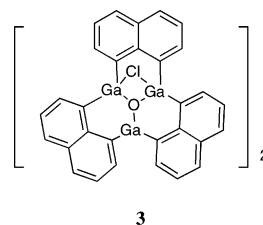
d_8 solution is bridged to a second moiety by the oxide atom,[67] represents a typical example. The data from both PGSE and variable-temperature proton NMR spectroscopic methods suggest that **3** is involved in a rapid monomer−dimer equilibrium.

In the titanium chemistry, shown below, addition of various quantities of the chelating ligand binol to the titanium(IV) tetrakis iso-propoxide complex affords two species, I and II.[68]
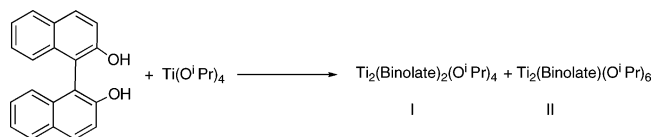
DOSY and T$_1$ measurements suggest that both are dinuclear; however, complex I is thought to contain two bridging binol moieties, that is, the binol bridges, rather than chelates, the two Ti atoms.

There are many examples of complexes of Ru(II) containing bridging halogen or other ligands. Sometimes the structure is obvious; for example, **4** has two
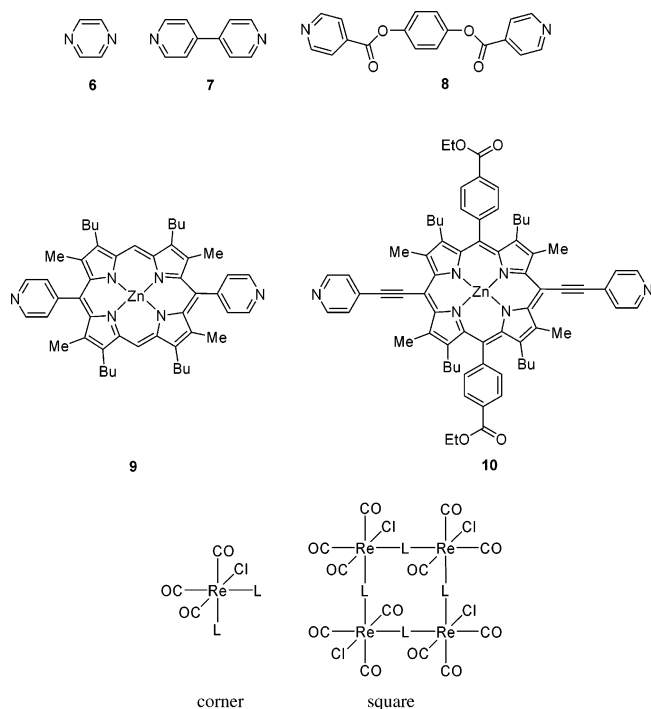

4   **5**
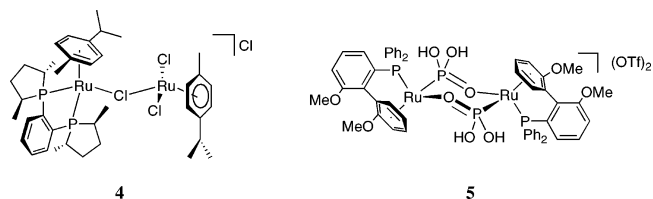
Table 2. Diffusion Data (10^{-10} m^2 s^{-1}) for the Ligands 6–10 and Their Re Complexes

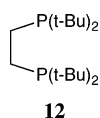| molecule	6	7	8	9	10
ligand	9.68 ± 0.09	6.03 ± 0.04	3.53 ± 0.04	2.24 ± 0.02	1.94 ± 0.06
corner	3.62 ± 0.08	2.69 ± 0.02	a	1.61 ± 0.03	a
square	2.37 ± 0.11	1.42 ± 0.05	0.87 ± 0.02	1.20 ± 0.04	1.04 ± 0.03

^{a} Not acquired.

different *p*-cymene ligands;[69] however, for **5**, the correct structure is not obvious.[70] In both cases, PGSE results have helped to confirm the presence of the higher molecular weight materials.

In this context, Larive and co-workers[71] recently used PGSE NMR measurements to characterize a series of large rhenium molecular species, which could not be characterized by mass spectroscopy. These rhenium complexes occur as both octahedral "corner" complexes and molecular "square" forms, which contain the ligands **6–10**. All of these mol-

ecules use the two remote pyridine nitrogen atoms to build up a series of new cluster molecules. A list of *D*-values for these Re clusters with ligands **6–10** can be found in Table 2. The complexes with the higher molecular weights result in lower *D*-values.

The solid-state structure[72] for the coordinatively unsaturated species [RuCl$_2$(CO)(d^{t}bpe)], **11**, containing the 1,2-bis di-*tert*-butylphosphinoethane chelate **12**, indicates a 16 e$^-$ Ru(II) species, perhaps stabi-


lized by an additional weak Ru$\cdots$H–C bond. However, low-temperature diffusion measurements[72] show that **11** is diffusing at a much slower rate than the coordinatively saturated model six-coordinate com-

Table 3. Diffusion Data (10^{-10} m^2 s^{-1}) for the Ru(II) Complexes (2 mM)

temp (K)	ion	D	r_H (Å)
223	[Ru(d^{t}bpe)(CO)Cl$_2$] **11**	2.23	6.8
223	Ru(d^{t}bpe)(CO)$_2$(Cl)$_2$ **13**	2.84	5.4

plex Ru(d^{t}bpe)(CO)$_2$(Cl)$_2$, **13**. The ratio of the *D*-values (**13/11** = 2.84/2.23, see Table 3) = 1.27 is in excellent agreement with a structure that has approximately double the molecular volume of **11**; that is, in solution, **11** is best described as having a halogen-bridged dinuclear structure.

Complexes of Cu(I) are well-known to form polynuclear materials,[73–76] although these species are not often found in connection with homogeneously catalyzed reactions. Using PGSE data, Pichota et al.[77] have shown that the isolated tetranuclear copper–thiolate clusters **15**, derived from **14**, are present
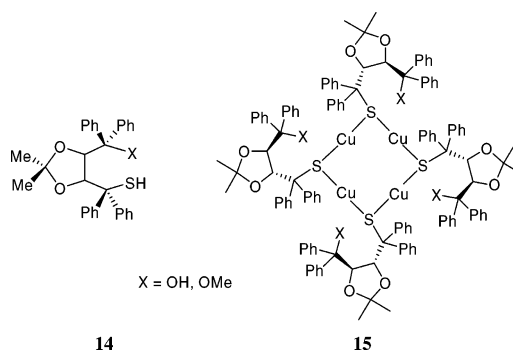
during the enantioselective copper-catalyzed 1,4-addition of nucleophiles to cyclic enones. Moreover, the diffusion results suggest that the cluster can add ligands, for example, a bulky isonitrile donor, without degrading the cluster structure.

Molecular sizes of aggregates of salt-free and salt-containing samples of dimethyl- (**16**) and bis[(trimethylsilyl)methyl]cuprates (**17**) have been deter-

minedby Xie et al.[78] using PGSE diffusion measurements (Figure 7). The diffusion coefficients indicate that the extent of aggregation depends on steric hindrance, salt effects, and sample concentrations.
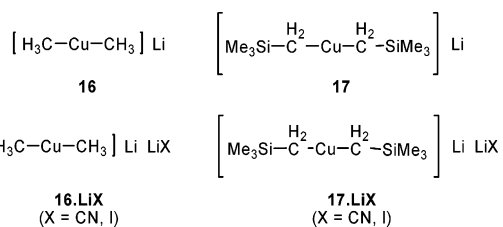
a)

b)
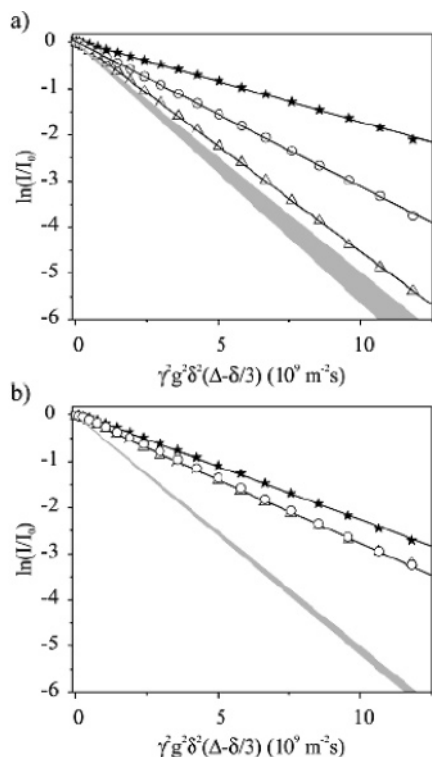
Figure 7. [1]H PGSE diffusion experiments in Et$_2$O at 239 K of (a) bis-[(trimethylsilyl)methyl]cuprates **17** [**17** (△), **17**·LiI (○), **17**·LiCN(∗)] and (b) dimethylcuprates **16** [**16** (△), **16**·LiI (○), **16**·LiCN(∗)]. The solid lines represent linear least-squares fits to the experimental data. The gray areas indicate the expected line positions if these species were to possess dinuclear structures.[78]

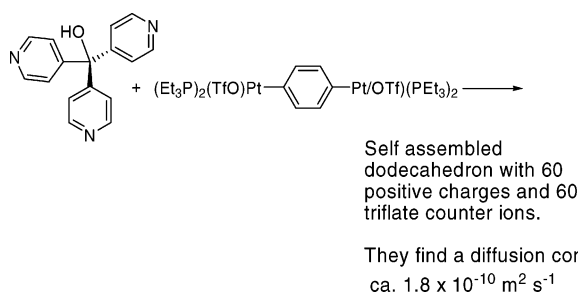The syntheses of several catenanes,[48] **18**, have been successfully achieved by reaction of the ethylenediamine nitrate complex, Pd(ONO$_2$)$_2$(en), with a bridging pyridine moiety in D$_2$O. These reorganization reactions to form catenanes of varying sizes (see the reaction below) have been studied via the DOSY methodology and reveal the presence of palladium catenanes with up to six metals and ligands. Although not all of these catenanes can be isolated, they can be recognized in solution.


Pd (catenanes), **18**   catenane fragment
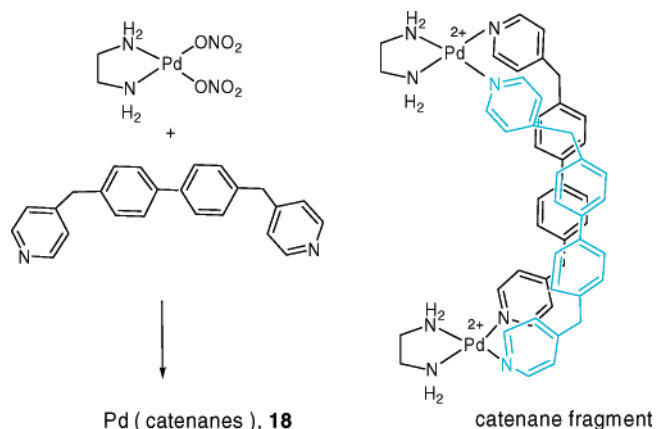
Moving from the catenanes to tin cluster chemistry, ^{1}H NMR PGSE spectroscopy has been applied in the study of the association behavior of the 12

tin oxo-cluster macrocation [(BuSn)$_{12}$(O)$_{14}$(OH)$_6$]$^{2+}$, **19**, with the two different and much smaller anions p-toluene sulfonate (PTS$^-$) and diphenylphosphinate (Ph$_2$PO$_2^-$).[20a] By monitoring the translational diffusion coefficients of the various species involved, it was shown that the degree of association depends on the anion involved and on the solvent used. When [(BuSn)$_{12}$(O)$_{14}$(OH)$_6$](PTS)$_2$ is mixed with 2 equiv of the salt [(NMe$_4$)(Ph$_2$PO$_2$)], the PTS$^-$ is displaced by the Ph$_2$PO$_2^-$, highlighting the greater affinity of the macrocation **19** for the Ph$_2$PO$_2^-$ anion.

Finally, in their construction of novel Pt molecules, Olenyuk et al.[79] have employed diffusion data to support a self-assembled dodecahedron structure of the product of the reaction shown below. The "square-like" materials, which are obtained, have hydrodynamic radii of the order of 5−7.5 nm.

+ (Et$_3$P)$_2$(TfO)Pt—⬡—Pt/OTf)(PEt$_3$)$_2$ ⟶

Self assembled dodecahedron with 60 positive charges and 60 triflate counter ions.

They find a diffusion constant of ca. 1.8 x 10^{-10} m^2 s^{-1}

Rounding off this section on the determination of molecular volumes, we note that several groups have used diffusion methods to estimate the size of dendrimeric materials. Gorman and co-workers[80] have studied the iron thiolate materials, **20**, and our

20
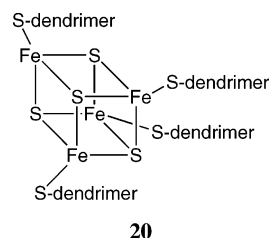
group has obtained PGSE data for the phosphine ligand set[81] **21**−**23**, shown in Scheme 2, as well as for the Pd(II) pincer derivatives **24** and **25**[82] in Scheme 3.

2.2. Hydrogen Bonding, Capsules, and Host−Guest Interactions

There are a number of ways in which the D-value for a small molecule (or small anion) can be influenced by the presence of another species: (a) hydrogen bonding, (b) host/guest encapsulation, and (c) ion pairing. Where strong hydrogen bonding exists, for example, the case of an anion bonding to an OH function associated with some part of a larger cation,[70] the relatively small anion translates at the rate of the larger cation. For this type of problem, one

Scheme 2. Phosphine Dendrimers 21−23

21	D = 4.67 (6)	r_H = 8.4 (1)
22	2.94 (6)	13.4 (1)
23	1.92 (6)	20.6 (1)

Scheme 3. Dendrimers Containing Pd(II) Pincers

24

25
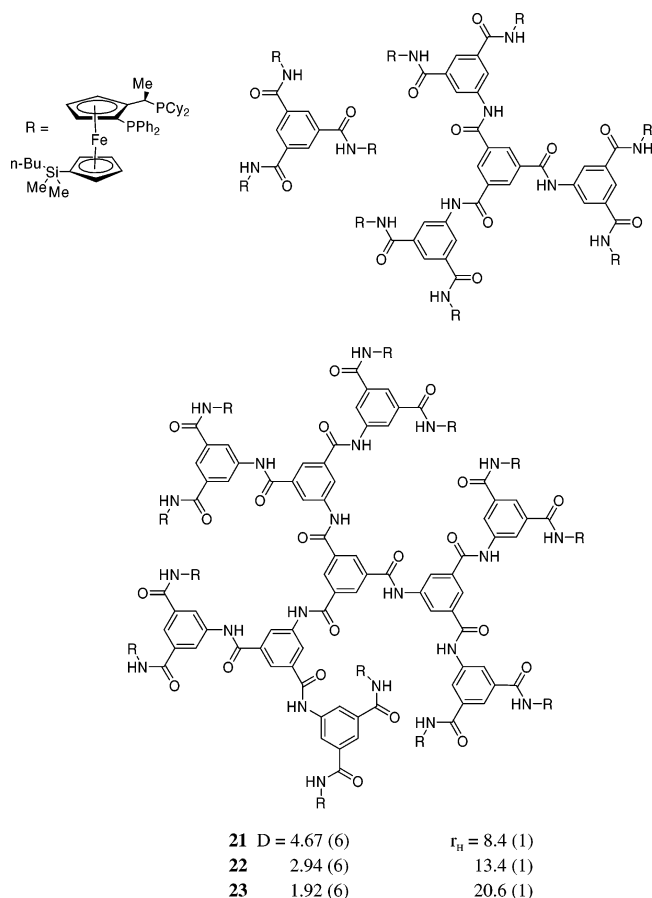
usually measures the *D*-value of the cation via ^{1}H NMR and that of the anion (BF$_4$, PF$_6$, CF$_3$SO$_3$, BArF, etc.) via ^{19}F NMR, although for tetraphenyl borate derivatives, that is, BPh$_4^−$ or BArF$^−$, ^{1}H NMR is also quite suitable.

Three examples involving H-bonding, **26**,[58] **28**,[83] and **29**,[84] in differing solvents are shown in Scheme 4. In all three salts, a hydroxyl function, either from a complexed al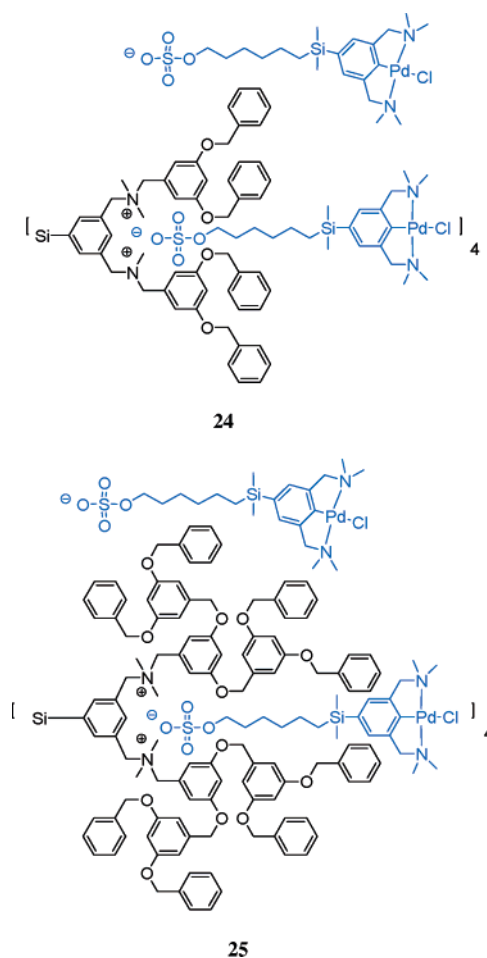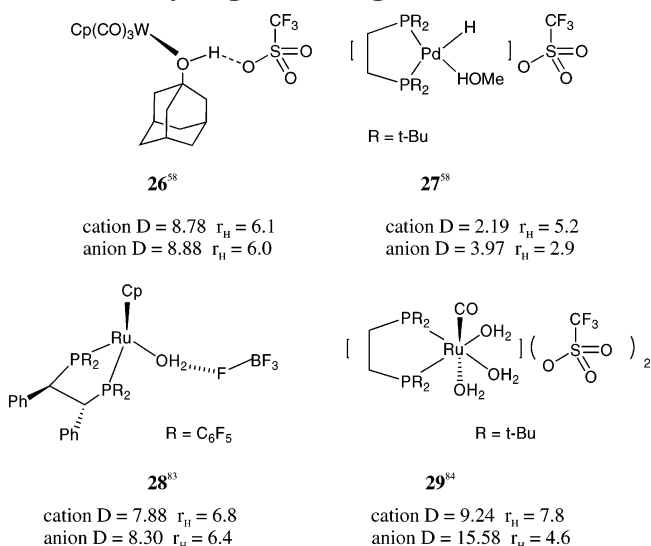cohol or bound water, hydrogen bonds to either the triflate or the tetrafluoroborate anion. When the anion is strongly held via the hydrogen bond, the translation rates (and thus the *D*-values, as measured by PGSE methods) decrease markedly and approach the observed *D*-values for the cations. The Ru(II) dinuclear complex, **5**, mentioned earlier offers a slight variation in that the triflate anion is involved in hydrogen bonding that stems from the various P(OH) moieties,[70] and not a routine alcohol hydroxyl group.

If equilibrium is established between the hydrogen-bound and free (solvated) anion, then the observed *D*-values for the ions represent an average, the magnitude of which provides an indication of the position of the equilibrium. If the cation is relatively large, for example, a transition metal complex possessing a large chiral auxiliary, the equilibrium will have a relatively large effect on the *D*-value for the anion but a much smaller effect on the cation. Interestingly, the Pd complex **27** was considered as possibly having a hydrogen bond from the bound methanol to the triflate anion; however, based

Scheme 4. Hydrogen Bonding and *D*-Values

26[58]	**27**[58]
cation D = 8.78 r_H = 6.1	cation D = 2.19 r_H = 5.2
anion D = 8.88 r_H = 6.0	anion D = 3.97 r_H = 2.9

28[83]	**29**[84]
cation D = 7.88 r_H = 6.8	cation D = 9.24 r_H = 7.8
anion D = 8.30 r_H = 6.4	anion D = 15.58 r_H = 4.6

on the diffusion data, this does not seem to be the case.[58]

Apart from electrostatic interactions, guest molecules and ions can be trapped or encapsulated in a host compound, and there are several nice examples of the use of diffusion data to recognize the capture of a small solvent guest molecule by a relatively large host.[62,63] The host compound may be a calixarene[62b,63] or a polyamide derivative[86] or even a

macrocyclic crown ether.[62,87] The principle is similar to that described above and often involves hydrogen bonding. When the guest is encapsulated, it translates relatively slowly and, consequently, reveals a smaller D-value. If the guest finds its way out of the host environment, its D-value rises markedly and approaches that of the "free" but solvated molecule.

The resorcinarene **30b** self-assembles spontaneously into a stable hexamer capsule in chloroform

30a R = CH$_3$

30b R= C$_{11}$H$_{23}$ D = 0.26-0.27 x 10^5 cm^{2}s^{-1};
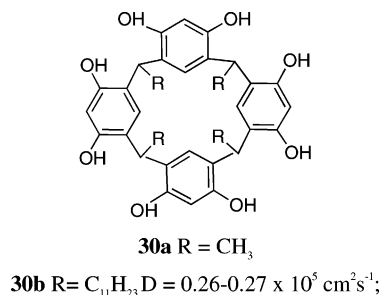
solution[62a] with a concomitant encapsulation of about eight CHCl$_3$ molecules. ^{1}H PGSE data give insight with respect to exchange phenomena and the translation of the encapsulated guest molecules. Somewhat unexpectedly, the encapsulated CHCl$_3$ molecules do not all have the same proton chemical shifts. The new guest environment may afford unexpected low-frequency ^{1}H chemical shifts (e.g., **30b**), and these can be a useful complement to the NMR diffusion data.

The tris(2-ureidobenzyl)amines, **31**, can self-assemble via hydrogen bonding to form new types of

31
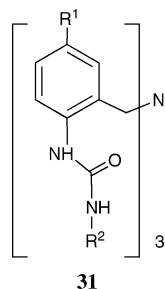
capped capsule-like dimeric aggregates derived from the flexible skeleton shown.[85] PGSE studies on these and related molecules reveal that they can take up small guest solvent molecules. The guest will take on the translational characteristics (D-value) of the host if it cannot readily escape from the capsule.

Frisch et al.[86] have recently demonstrated that the affinity of the cobaltocenium cation **32** for a host related to **31** is at least 5 orders of magnitude larger than that of ferrocene, **33**. The DOSY spectrum shown in Figure 8 nicely demonstrates the different interactions and, specifically, that the ferrocene is moving much faster.

The macrocyclic alkoxide complex **34** offers a nice example of the use of multinuclear diffusion methods.[87] The ligand (^{1}H), the lithium (^{7}Li), and the anion

32   **33**
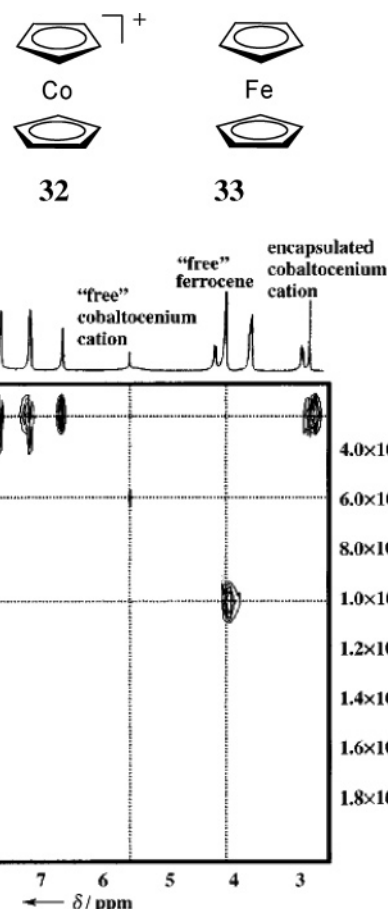
Figure 8. The DOSY spectrum[86] (400 MHz, 298 K) of a solution containing ferrocene and cobaltocenium cation in C$_2$D$_4$Cl$_2$. The signal at δ = 2.72 ppm represents the encapsulated cobaltocenium cation, which has the same diffusion coefficient as all the signals of the tetraureacalix-[4]arene dimer. The signals of the free ferrocene and cobaltocenium cation at δ = 4.06 and 5.61 ppm, respectively, were found to have much higher diffusion coefficients.

(^{19}F) are all translating at the same rate, thereby indicating that the BF$_4$ anion is strongly associated with the complexed lithium cation.
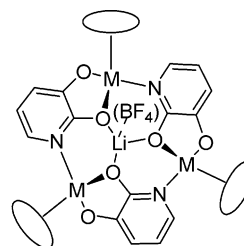
34, M = Ru, ^{7}Li D = 8.26; ^{19}F, D = 8.22; ^{1}H, D = 8.22

(2 mM solutions, units are x 10^{-10} m^2 s^{-1})

Although the examples described above are illustrative, the individual D-values are sometimes difficult to appreciate. Consequently, for a selection of transition metal complexes, we have begun to

Scheme 5. D (10^{-10} m^2 s^{-1}) and r_H (Å) Values for 35−40 in CDCl$_3$[88]


35	36	37
6.21 (6) 6.3 (1)	8.47 (6) 4.7 (1)	7.33 (6) 5.4 (1)
38	39	40
8.37 (6) 4.8(1)	7.37 (6) 5.4 (1)	6.78 (6) 5.8 (1)

Table 4. ^{1}H, ^{31}P, and ^{19}F Diffusion Constants (10^{-10} m^2 s^{-1})^a and r_H Values (Å)

compd	X	aryl Y	D (^{1}H)	r_H
		L = PEt$_3$		
41a	Br	C$_6$H$_5$	12.01	4.5
41b	Br	C$_6$H$_4$(m-CF$_3$)	11.70^b	4.6
41c	Br	C$_6$H$_4$(p-CF$_3$)	11.41^c	4.7
41d	Br	C$_6$H$_4$(m-Br)	11.45	4.7
41e	Br	C$_6$H$_4$(p-Br)	11.34	4.7
41f	Br	C$_6$H$_4$(m-OCH$_3$)	11.39	4.7
41g	Br	C$_6$H$_4$(p-OCH$_3$)	11.29	4.7
41h	Br	C$_6$H$_4$(p-NMe$_2$)	11.15	4.8
42	Cl	C$_6$H$_5$		
		L = PPh$_3$		
			11.99	4.5
43	Cl	C$_6$H$_5$	9.12	5.8

^{a} 2 mM in CD$_2$Cl$_2$. ^{b} D(^{19}F) = 11.89 (10 mM); r_H = 4.4. ^{c} D(^{19}F) = 11.60 (10 mM); r_H = 4.5.

Table 5. ^{1}H Diffusion Constants (10^{-10} m^2 s^{-1})^a and r_H Values (Å)

compd	L^1	L^2	D (^{1}H)	r_H
44a	PPh$_3$	PPh$_3$	8.86	6.0
44b	P(p-Tol)$_3$	P(p-Tol)$_3$	8.18	6.6
44c	PPh$_2$Bz	PPh$_2$Bz	7.94	6.8
44d	AsPh$_3$	AsPh$_3$	9.30	5.8
44e	AsPh$_2$Me	AsPh$_2$Me	9.98	5.4
44f	AsPh$_2$Me	PPh$_2$Bz	9.28	5.8
44g	P[OCH(CH$_3$)$_2$]$_3$	P[OCH(CH$_3$)$_2$]$_3$	10.35	5.2
44h	NH$_2$(CH$_2$)$_5$CH$_3$	DMSO	11.79	4.5
44i^b	^{15}NH$_2$(CH$_2$)$_5$CH$_3$	DMSO	11.95	4.5
44j	2-picoline	DMSO	12.18	4.4
44k	3-picoline	DMSO	12.24	4.4
44l	4-picoline	DMSO	11.94	4.5
44m	3-picoline	3-picoline	11.52	4.7

^{a} 2 mM in CD$_2$Cl$_2$. ^{b} ^1J(^{15}N,^{1}H) = 72 Hz.
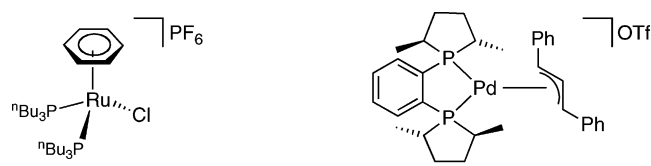
Scheme 6. Cycloplatinated Salicylaldehyde Complexes

	L^1	L^2
44a	PPh$_3$	PPh$_3$
44b	P(p-Tol)$_3$	P(p-Tol)$_3$
44c	PPh$_2$Bz	PPh$_2$Bz
44d	AsPh$_3$	AsPh$_3$
44e	AsPh$_2$Me	AsPh$_2$Me
44f	AsPh$_2$Me	PPh$_2$Bz
44g	P[OCH(CH$_3$)$_2$]$_3$	P[OCH(CH$_3$)$_2$]$_3$
44h	NH$_2$(CH$_2$)$_5$CH$_3$	DMSO
44i	^{15}NH$_2$(CH$_2$)$_5$CH$_3$	DMSO
44j	2-picoline	DMSO
44k	3-picoline	DMSO
44l	4-picoline	DMSO
44m	3-picoline	3-picoline

collect a small library of D and r_H values. Scheme 5 shows diffusion data for a small selection of Pd complexes,[88] **35−40**, and Tables 4 and 5 give data for some platinum phosphine complexes, *trans*-PtX-(aryl)(L)$_2$, **41−43**, and a series of cycloplatinated
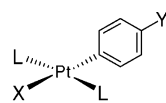
41, L = PEt$_3$, X = Br
42, L = PEt$_3$ X = Cl
43, L = PPh$_3$, X = Cl

salicylaldehyde complexes, **44**, respectively, in dichloromethane solution[54] (see Scheme 6).

2.3. Ion Pairing

Although conductivity measurements still represent an accepted method of measuring how ions interact, we have shown that the individual D-values for the ions of a given salt can provide a useful alternative. This is especially true when taken together with HOESY (hetero-nuclear Overhauser spectroscopy) or NOESY measurements or both.

The solvent dependence[81,88] of the ^{1}H and ^{19}F D-values for the Ru(II) and Pd(II) salts **45** and **46**,

45	**46**
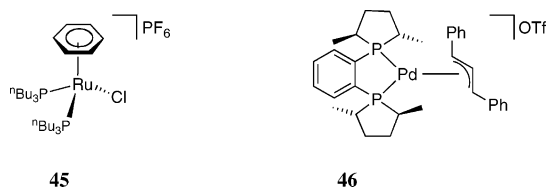
respectively, are illustrative (see Table 6). In chloroform solution, the anions and cations of **45** and **46** are moving at about the same rate, based on their respective D-values, suggesting that a tight ion pair represents the correct description for these salts (i.e., 100% for **45** and almost 100% for **46**). However, in dichloromethane solution, the cations and anions have significantly different D-values, although the resulting r_H values still suggest a relatively large amount of ion pairing. The suggestion that there is a "relatively large" contribution from ion pairing in dichloromethane derives from the knowledge that the PF$_6^-$ and OTf$^-$ anions are known[52,58,83,84] to have diffusion-based r_H values in methanol (a strongly sol-

Table 6. D (10^{-10} m^2 s^{-1}) and r_H Values for Cation and Counterion in CDCl$_3$ and CD$_2$Cl$_2$ of 45 and 46

compd	solvent	fragment	D^a	$r_H{}^b$ (Å)
45	CDCl$_3$	cation^c	6.25(6)^d	6.3(1)^d
	CDCl$_3$	PF$_6{}^e$	6.27(6)	6.3(1)
	CD$_2$Cl$_2$	cation^c	8.74(6)	6.2(1)
	CD$_2$Cl$_2$	PF$_6{}^e$	10.17(6)	5.3(1)
46	CDCl$_3$	cation^c	6.64(6)	6.0(1)
	CDCl$_3$	OTf^e	6.45(6)	6.1(1)
	CD$_2$Cl$_2$	cation^c	9.14(6)	5.9(1)
	CD$_2$Cl$_2$	OTf^e	11.69(6)	4.7(1)

^{a} Estimated using the diffusion coefficient of HDO in D$_2$O as in ref 88. ^{b} η (CDCl$_3$) = 0.55 × 10^{-3} kg s^{-1} m^{-1}; η(CD$_2$CL$_2$) = 0.40 × 10^{-3} kg s^{-1} m^{-1}. ^{c} Using ^{1}H signals. ^{d} Standard deviation. ^{e} Using ^{19}F resonance.

vating solvent) of ca. 2.6 and 3.2 Å, respectively. Consequently, we interpret the r_H values of 5.3 and 4.7 Å for the PF$_6{}^-$ and OTf$^-$ anions, respectively, as arising from significant but not complete ion pairing. Although many salts are strongly solvated in methanol, one cannot exclude some ion pairing in this solvent.[89,90]

It would seem that in chloroform solution, strong ion pairing is favored. The analogous diffusion measurements for the Pd salts **47−50** in chloroform (see
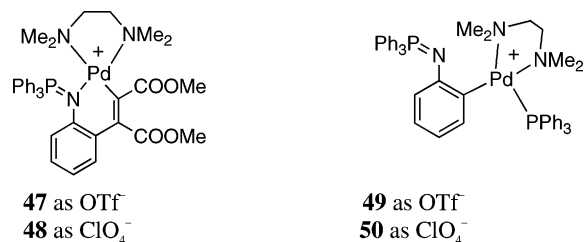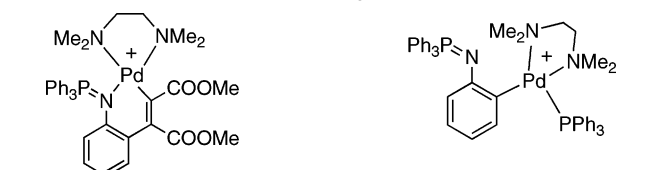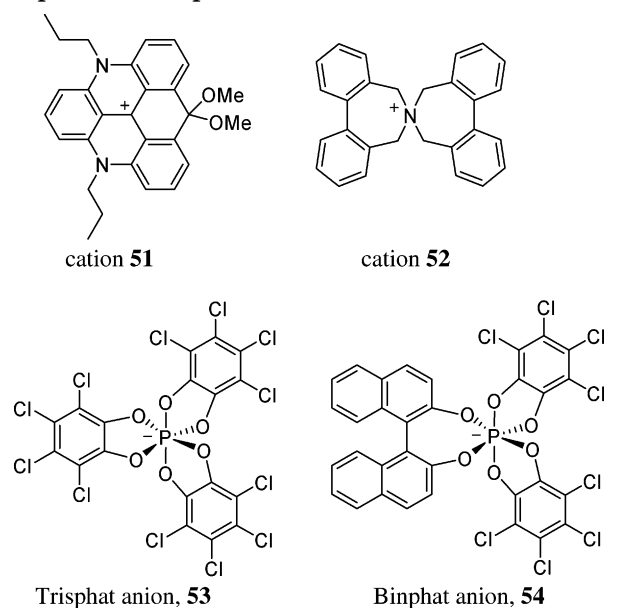

47 as OTf$^-$
48 as ClO$_4{}^-$
49 as OTf$^-$
50 as ClO$_4{}^-$

Table 7), reveal equivalent D-values for the two triflate salts (D = 6.27(6) (^{1}H) and D = 6.17(6) (^{19}F) for the two ions of **47** and D = 5.98(6) (^{1}H) and D = 6.11(6) (^{19}F) for the two ions of **49**) and very strong but not quite complete ion pairing for the two perchlorate salts.[52] The poor sensitivity in the mea-

Table 7. D Values (10^{-10} m^2 s^{-1}) for the Palladium Salts 47−50 (9.0 mM) in CDCl$_3$

47 as OTf$^-$
48 as ClO$_4{}^-$
49 as OTf$^-$
50 as ClO$_4{}^-$

	47	**48**	**49**	**50**
cation	6.27(6) (^{1}H)	5.79(6) (^{1}H)	5.98(6) (^{1}H)	5.69(6) (^{1}H)
anion	6.17(6) (^{19}F)	6.51(6) (^{35}Cl)	6.11(6) (^{19}F)	7.19(6) (^{35}Cl)

surement of the Cl resonance required a somewhat larger concentration (9 mM) than normal (1−2 mM).

This type of solvent dependence of the ion pairing is not limited to salts of transition metals. Table 8

Table 8. D (10^{-10} m^2 s^{-1}) and r_H (Å)$^{a-c}$ Values for Trisphat and Binphat Salts

cation **51**   cation **52**

Trisphat anion, **53**   Binphat anion, **54**

salt	concn (mM)	fragment^c	CDCl$_3$ D	CDCl$_3$ r_H	CD$_2$Cl$_2$ D	CD$_2$Cl$_2$ r_H
(51)(53)	10	cation	5.05	8.1	8.71	6.1
		anion (^{31}P)	5.21	7.9	8.29	6.4
	5	cation	5.41	7.7	8.60	6.2
		anion				
	1	cation	5.64	7.3	9.00	5.9
		anion				
(51)(54)	10	cation	4.67	8.9	8.08	6.5
		anion	4.66	8.9	7.10	7.5
	5	cation	4.91	8.5	8.11	6.6
		anion	4.92	8.4	7.17	7.5
	1	cation	5.40	7.7	8.88	5.9
		anion	5.33	7.8	7.61	6.9
(51)(PF$_6$)	10	cation			9.70	5.4
		anion (^{19}F)			13.5	3.9
	5	cation			9.70	5.4
		anion (^{19}F)			13.9	3.8
	1	cation			10.0	5.3
		anion (^{19}F)			14.8	3.6
(52)(53)	5	cation	5.38	7.6	8.99	5.9
		anion (^{19}F)	5.50	7.5	7.90	6.7
	1	cation	5.68	7.2	9.57	5.5
		anion (^{31}P)				
(52)(54)	5	cation				
		anion	5.17	8.0	7.19	7.4
	5 (229 K)	cation	1.57	7.9	2.85	6.1
		cation	1.56	8.0	2.68	6.5
		anion	1.58	7.9	2.34	7.4
	1	cation				
		anion	5.65	7.3	7.73	6.8
(52)(PF$_6$)	5	cation			10.3	5.1
		anion (^{19}F)			12.8	4.1
	1	cation			10.7	4.9
		anion (^{19}F)	7.84	5.2	13.5	3.9

^{a} Standard deviation = ±0.06 × 10^{-10} m^2 s^{-1} for D-values and ±0.1 Å for r_H values. ^{b} For the calculation of r_H, the viscosity of the nondeuterated solvent at the temperature of the measurements (229, 299, or 300 K) was used. The values at 229 K are 1.35 × 10^{-3} kg s^{-1} m^{-1} for CHCl$_3$ and 0.964 × 10^{-3} kg s^{-1} m^{-1} for CH$_2$Cl$_2$. ^{c} When not otherwise specified, the measurements were carried out using the ^{1}H NMR resonances.

shows the D and r_H values for two organic cations, **51** and **52**, which are paired with the relatively large chiral trisphat and binphat anions,[55] **53** and **54**, respectively, developed by Lacour and co-workers[91−93] (see Scheme 7). Obviously, in chloroform solution,

Scheme 7. The Chiral Cations and Phosphate Anions[55]

cation **51**   cation **52**

Trisphat anion, **53**   Binphat anion, **54**
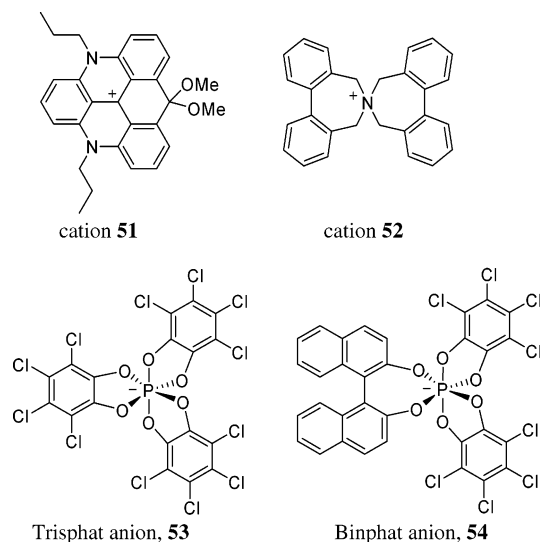
strong ion pairing is, once again, favored. For the binphat salt, (**52**)(**54**), the ^{1}H, ^{19}F, and ^{31}P PGSE diffusion studies reveal the first example of the dependence of a diffusion value on diastereomeric structure (see Figure 9).[55] Clearly, the ability to
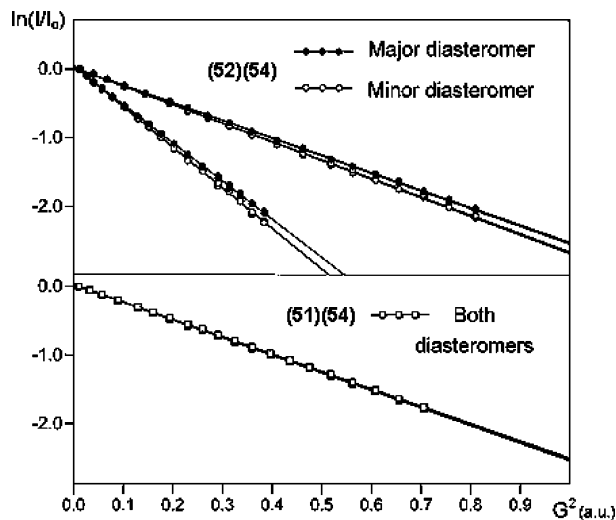
Figure 9. Plot of $\ln(I/I_0)$ vs arbitrary units proportional to the square of the gradient amplitude for ^{1}H PGSE diffusion measurements on the cations of (top) (**52**)(**54**), and (bottom) (**51**)(**54**) in CD_2Cl_2. The differences in D between the diastereomers for (**52**)(**54**) are visible, whereas the two diastereomers for (**51**)(**54**) diffuse identically. The results of two different measurements on (**52**)(**54**) with different NMR parameters are shown. Both were carried out at 229 K. Each line results from the overlapping of measurements on two resonances of the corresponding diastereomer.[55]

measure the diffusion rates for the cation and anion separately, that is, multinuclear PGSE studies, rep-

resents a powerful tool, and readily affords a qualitative view of the ion pairing.[94]

The data in Table 8 reveal a concentration dependence of the D-values, and this has been observed by several groups.[66,88] In our experience, in the range 1−10 mM, a 5−10% variance in D-value is not unusual. Often one finds that the D-value increases with decreasing concentration. This dependence might arise due to (a) a change in the aggregation state,[95] (b) a change in the ion pairing, or (c) a change in the solution viscosity (and naturally, a mixture of all of these effects). However, the data in Table 9 show that this concentration dependence is

Table 9. D Values (10^{-10} m^2 s^{-1}) for Complexes 55 and 56 in CDCl$_3$ at Different Concentrations[88]

55   **56**

	concn (mg/g)	D
55	1.3	6.74(6)
55	7.4	6.82(6)
55	14.8	6.72(6)
56	0.8	6.50(6)
56	6.6	6.12(6)
56	13.2	5.94(6)

usually greater for charged species,[88] such as the Ru(II) salt **56**, than for the neutral halogen-bridged

55   **56**
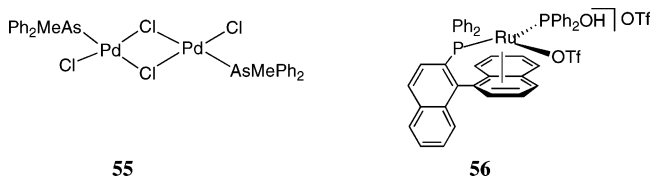
Pd(II) dinuclear complex **55**, where the magnitude of the effect for D falls within the experimental error.

Tables 10 and 11, from Macchioni and co-workers,[66] give extensive diffusion results from a series of (mostly) zirconium catalyst precursors. The tables show diffusion coefficients, D, at various concentrations, *corrected* diffusion coefficients, D^*, based on measurements from model silicon compounds, for example, Si(p-tolyl)$_4$ (TPTS),[66] and corrected coefficients, c, from the Stokes−Einstein equation, that is, the value "6" is not uniformly used.[50]

Specifically, for the Zr(IV) salts labeled **A−D** in Table 10, one finds that the complexes all show invariant apparent molecular volumes, that is, very similar r_H values, over a wide range of concentrations. These results are considered to be consistent with inner sphere ion pairs. Returning to the concentration effect, Table 11 clearly shows the expected increase in D value with decreasing concentration, and this has been attributed to the formation of ion quadrupoles or even higher aggregates.

Table 10. Diffusion Coefficients (10^{-10} m^2 s^{-1}), Corrected Diffusion Coefficients^a (D*), ^{a}Hydrodynamic Radii (r_H, Å), and c Factor[50] Values at Various Concentrations (10^{-3} M) for the Standards, the Neutral Metallocenium Precursors, and the Products[66]

	concn	D	D (TPTS)	D*	r_H	c
Si(p-Tol)$_4$ (TPTS)	0.10	8.31			4.66	5.0
Si[Si(CH$_3$)$_3$]$_4$ (TMSS)	0.10	11.2			3.80	4.5
(Me$_5$Cp)$_2$ZrMe$_2$	0.10	10.1			4.06	4.7
Cp$_2$ZrMe$_2$	0.10	12.2			3.63	4.4
(Me$_5$Cp)TiMe$_3$	9.75	11.8	8.20	12.0	3.64	4.4
Me$_2$C(fluorenyl)(Cp)ZrMe$_2$	2.46	9.44	7.94	9.89	4.13	4.7
Me$_2$Si(Me$_4$Cp)(t-BuN)ZrMe$_2$	8.74	9.92	7.77	10.6	3.94	4.6
Me$_2$C(fluorenyl)(Cp)Zr(CH$_2$Ph)$_2$	2.00	7.69	7.77	8.23	4.70	5.0
(Me$_5$Cp)$_2$ZrMe$_2$	7.34	9.63	8.02	9.97	4.11	4.7
Cp$_2$ZrMe$_2$	15.67	11.1	7.11	12.9	3.47	4.3
[Me$_2$Si(Me$_4$Cp)(t-BuN)TiMe] + [MeB(C$_6$F$_5$)$_3$]	9.90	6.86	7.79	7.32	5.12	5.1
[Me$_2$C(fluorenyl)(Cp)ZrMe] + [MeB(C$_6$F$_5$)$_3$]	4.80	6.64	7.66	7.20	5.1	5.2
[(Me$_5$Cp)$_2$ThMe] + [B(C$_6$F$_5$)$_4$]	0.80	6.62	8.02	6.85	5.39	5.2
[Cp$_2$ZrMe] + [MeB(C$_6$F$_5$)$_3$]	2.50	7.08	7.63	7.71	4.92	5.1
A [(Me$_2$Cp)$_2$ZrMe] + [MeB(C$_6$F$_5$)$_3$]	5.00	6.92	7.61	7.56	5.00	5.1
	1.00	6.72	7.40	7.56	5.00	5.1
B [(Me$_2$SiCp)$_2$ZrMe] + [MeB(C$_6$F$_5$)$_3$]	8.60	6.53	7.27	7.46	5.05	5.1
	2.80	6.55	7.21	7.55	5.00	5.1
	1.37	6.58	7.24	7.56	5.00	5.1
	0.68	6.81	7.42	7.63	4.97	5.1
C [Me$_2$C(fluorenyl)(Cp)ZrMe] + [FPBA]	5.00	5.34	7.03	6.31	5.76	5.3
	2.80	5.76	7.54	6.35	5.72	5.3
	1.15	6.20	8.08	6.38	5.70	5.3
D [C$_2$H$_4$(indenyl)$_2$ZrMe] + [FPBA]	3.50	6.00	7.82	6.37	5.70	5.3
	2.05	5.40	7.07	6.35	5.72	5.3

^{a} The corrected D* values correspond to a hypothetical measurement carried out at 22 °C in a solution containing the reported nominal concentration but having the viscosity of pure C$_6$D$_6$. The "c" values have been corrected from the usual value of "6" using a literature suggestion.[49,50]

Table 11. Diffusion Coefficients (10^{-10} m^2 s^{-1}), Corrected Diffusion Coefficients^a (D*), Hydrodynamic Radii (r_H, Å), and c Factor Values at Different Concentrations (10^{-3} M)[66]

concn	D	D (TPTS)	D*	r_H	c	concn	D	D (TPTS)	D*	r_H	c
[(Me$_2$SiCp)$_2$Zr(Me)(THF)] + [MeB(C$_6$F$_5$)$_3$]
2.20	5.17	7.45	5.76	6.19	5.4	0.99	6.01	7.59	6.57	5.57	5.3
1.70	5.76	7.98	6.00	5.99	5.4	0.90	5.93	7.42	6.65	5.52	5.3
1.60	4.87	6.67	6.07	5.94	5.4	0.70	6.20	7.36	7.00	5.30	5.2
1.20	5.76	7.55	6.34	5.73	5.3	0.09	6.74	7.71	7.27	5.15	5.2
[(Me$_2$SiCp)$_2$Zr(Me)(PPh$_3$)] + [MeB(C$_6$F$_5$)$_3$]
3.10	4.11	7.20	4.74	7.30	5.6	0.91	4.96	7.18	5.73	6.22	5.4
2.35	4.29	7.21	4.95	7.03	5.5	0.86	5.36	7.67	5.81	6.15	5.4
1.40	4.93	7.53	5.44	6.50	5.5	0.45	5.80	7.50	6.43	5.67	5.3
1.05	5.06	7.44	5.66	6.29	5.4	0.12	5.85	7.65	6.36	5.72	5.3
[(Me$_2$SiCp)$_2$Zr(Me)(THF)] + [B(C$_6$F$_5$)$_4$]
1.48	5.15	7.74	5.53	6.40	5.5	0.38	6.37	7.86	6.73	5.47	5.2
0.82	5.88	7.70	6.34	5.73	5.3						
[Me$_2$Si(Me$_4$Cp)(t-BuN)Zr(Me)(C$_6$D$_6$)] + [B(C$_6$F$_5$)$_4$]
0.64	5.04	7.20	5.81	6.15	5.4	0.24	5.64	7.28	6.43	5.66	5.3
0.42	5.38	7.19	6.22	5.82	5.3	0.12	5.73	7.30	6.53	5.60	5.3
[Cp$_2$ZrMe)$_2$(μ-Me)] + [MePBB]
5.20	4.50	7.35	5.09	6.87	5.5	0.97	4.85	7.00	5.76	6.19	5.4
3.30	4.22	6.79	5.17	6.78	5.5	0.55	5.02	7.06	5.91	6.07	5.4
2.00	4.58	7.00	5.44	6.49	5.5	0.11	5.15	7.01	6.11	5.90	5.4

^{a} The corrected D* value corresponds to a hypothetical measurement carried out at 22 °C in a solution containing the reported nominal concentration but having the viscosity of pure C$_6$D$_6$.

Figure 10 shows PGSE results for LiPPh$_2$ in THF and Et$_2$O solutions.[53] In THF, LiPPh$_2$ exists as a mononuclear solvated species, whereas in Et$_2$O, a dinuclear structure is proven; however, equally interesting is the solvent and temperature dependence of the ion pairing (see Table 12[53]). For LiPPh$_2$ at ambient temperature, there is strong ion pairing in ether and less than 100% ion pairing in THF. However, at 155 K, there is strong ion pairing in THF! The explanation for this observation seems less

than obvious because it suggests that increasing the temperature promotes ion pairing. Moreover, for trityllithium, **57**, and fluorenyllithium, **59**, (see Scheme 8) it is also the case that ion pairing is favored at 299 K but that the ions are well separated at 155 K.[53] The scheme also shows several other organometallic lithium derivatives, **57**–**64**, for which PGSE data have been obtained (see Tables 13 and 14). For 2-lithio-1,3-dithiane, **63**, and lithium hexamethyldisilazane (LiHMDS), **64**, low-temperature data show
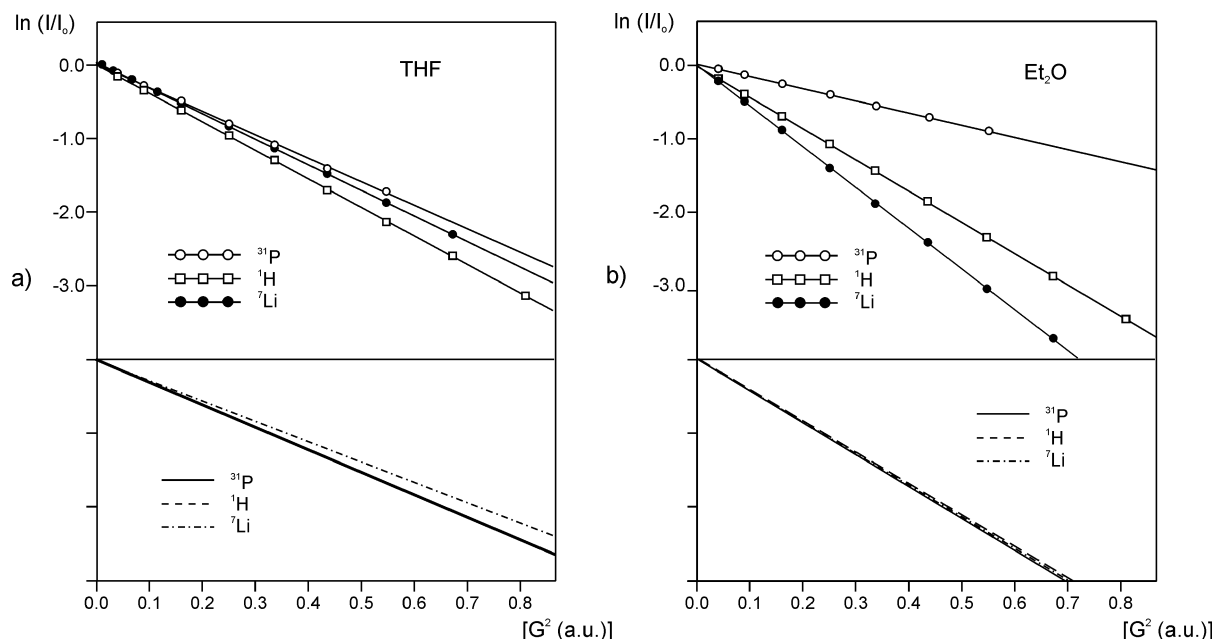
Figure 10. Plot of the $\ln(I/I_0)$ vs arbitrary units proportional to the square of the gradient amplitude for ^{1}H, ^{7}Li, and ^{31}P PGSE diffusion measurements on 60 mM Ph$_2$PLi samples at RT in (a) THF and (b) Et$_2$O. The observed intensity attenuation depends on the D-values, the gyromagnetic ratio (γ) of the observed nucleus, and the diffusion parameters. The lower sections of the panels show the calculated lines adjusted to a hypothetical unified set of parameters, and in Et$_2$O, the slopes[53] are equal for the three measurements.

Table 12. D (10^{-10} m^2 s^{-1}) and r_H (Å) Values^a in THF and Et$_2$O at RT and in THF at 155 K and Et$_2$O at 202 K^b

THF and Et$_2$O at RT				
	nucleus	D^c	$r_H{}^d$	$(r_H)^e$
LiPPh$_2$ (THF)	^{7}Li	10.1	4.7	(5.6)
	^{1}H	11.0	4.3	(5.2)
	^{31}P	11.0	4.3	(5.2)
LiPPh$_2$ (Et$_2$O)	^{7}Li	16.1	6.2	(6.7)
	^{1}H	16.0	6.2	(6.7)
	^{31}P	16.2	6.1	(6.7)
Ph$_2$PH (THF)	^{31}P	15.8	3.0	(4.5)
	^{1}H	15.8	3.0	(4.5)

THF (155 K) and Et$_2$O (202 K)			
	nucleus	D	$r_H{}^f$
LiPPh$_2$ (THF)	^{7}Li	0.221	4.9
	^{31}P	0.242	4.5
	^{1}H	0.239	4.5
Ph$_2$PH (THF)	^{31}P	0.380	2.9
	^{1}H	0.386	2.9
TMSS (THF)	^{1}H	0.233^g	4.3
LiPPh$_2$ (Et$_2$O)	^{7}Li	h	h
	^{1}H	2.78^i	6.6
TMSS (Et$_2$O)	^{1}H	4.47^j	4.1

^{a} All at 60 mM. ^{b} At 155 K, the LiPPh$_2$ precipitates from Et$_2$O solution. ^{c} Experimental error is ca. $\pm$2%. ^{d} Standard deviation is ca. $\pm$0.1 Å. η(THF, 299 K) = 0.461 $\times$ 10^{-3} kg s^{-1} m^{-1}. η(Et$_2$O, 299 K) = 0.221 $\times$ 10^{-3} kg s^{-1} m^{-1}. ^{e} These eight r_H-values have been calculated using the constants 5.0, 5.5, and 4.0 (instead of 6) for LiPPh$_2$ (THF), LiPPh$_2$ (Et$_2$O), and HPPh$_2$, respectively.[50] ^{f} Standard deviation is ca. $\pm$0.1 Å. ^{g} Room-temperature values are D = 10.9 $\times$ 10^{-10} m^2 s^{-1} and r_H = 4.3 Å. ^{h} Not measurable. ^{i} A coaxial NMR tube (ID = 1.96 mm; OD = 2.97 mm) separated by a spacer was used. See ref 58. ^{j} Room-temperature values are D = 24.2 $\times$ 10^{-10} m^2 s^{-1} and r_H = 4.1 Å. Estimated viscosities are η(THF, 155 K) = 10.4 $\times$ 10^{-3} kg s^{-1} m^{-1} and η(Et$_2$O, 202 K) = 0.807 $\times$ 10^{-3} kg s^{-1} m^{-1}.

that the ions remain together. However, for **63**, a mononuclear species has been established, whereas

Scheme 8. Lithium Salts and Anions, 57–64, in the PGSE Study
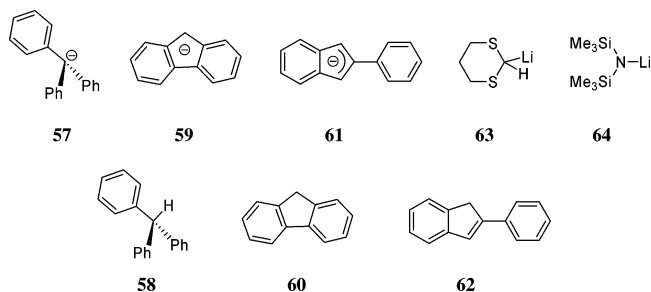
for the lithium amide **64**, the PGSE results allow two different aggregation states to be readily recognized.[96]

The studies for these various lithium salts nicely show that PGSE methods are quite useful for recognizing ion pairing (or the lack thereof) and aggregation in main group salts; however, the explanation for the observed temperature dependence of the ion pairing is not completely clear. Interestingly, it is known[97] that the dielectric constant of THF increases markedly (more than doubles!) on cooling from ambient temperature to 155 K. Consequently, we assign the observation of the separated ions at 155 K to a marked increase in the stability of the separated ions, due to increased solvation.[96] Given how often salts are crystallized at low temperature and how frequently NMR data are recorded at very low temperature, these new PGSE data are thought provoking.

Cohen et al.[64b,c] have reported ^{1}H diffusion data for a series of lithium and sodium salts of organic polycyclic systems and, for several examples, attributed the data to ion pairing effects.

Before moving on to applications in homogeneous catalysis, the PGSE (and Overhauser NMR data) for the three salts [Rh(1,5-COD)(Biphemp)]X, Biphemp

Table 13. D (10^{-10} m² s⁻¹) and r_H (Å) Values[a] for the Lithium Salts in THF at 299 K

	nucleus	D^c	$r_H{}^d$	r^e	δ (⁷Li)	$\Delta\nu_{1/2}$
LiCPh₃, **57**	⁷Li	7.40	6.4		−0.45	10.2
	¹H	7.38	6.4			
HCPh₃, **58**	¹H	12.5	3.8	4.0		
LiFlu, **59**	⁷Li	8.85	5.4		−1.44	13.8
	¹H	8.81	5.4			
HFlu, **60**	¹H	17.44	2.7	3.2		
LiInd, **61**	⁷Li	8.89	5.3		−3.24	5.0
	¹H	9.16	5.2			
HInd, **62**	¹H	15.96	3.0	3.9		
HDith	¹H	20.17	2.4	2.6		
LiHMDS, **64**	⁷Li	11.4	4.2		0.78	11.0
60 mM	¹H	11.3	4.2			
LiHMDS, **64**[f]	⁷Li	9.51	5.0		1.10	32.6
600 mM	¹H	9.55	5.0			
HMDS		16.7	2.8	3.2		
TMSS		10.9	4.3	4.4		

[a] All at 60 mM. [b] η(THF, 299 K) = 0.461 × 10⁻³ kg s⁻¹. [c] Experimental error is ca. ±2%. [d] Standard deviation is ca. ±0.1 Å. [e] Estimated using ChemBats3D by averaging the distances between the centroid and the outer hydrogen. [f] Measurements achieved in a 0.6 M sample using a coaxial NMR tube (ID = 1.96 mm; OD = 2.97 mm) separated by a spacer. See ref 58.

Table 14. D (10^{-10} m² s⁻¹) and r_H (Å) Values[a] for the Lithium Salts in THF at 155 K

	nucleus	D^b	$r_H{}^c$	r^d	δ (⁷Li)	$\Delta\nu_{1/2}$
LiCPh₃, **57**	⁷Li	0.224	4.9		−0.41	2.6
	¹H	0.258	4.2			
HCPh₃, **58**	¹H	0.282	3.9	4.0		
LiFlu, **59**	⁷Li	0.223	4.9		−1.13	2.8
	¹H	0.253	4.3			
HFlu, **60**	¹H	0.396	2.8			
LiDith, **63**[e]	⁷Li	5.23	4.4		0.11	3.6
252 K	¹H	5.22	4.4			
HDith[e]	¹H	9.31	2.4	2.6		
252 K						
LiDith, **63**	⁷Li	f				
	¹H	0.245	4.5			
HDith	¹H	0.447	2.4	2.6		
LiHMDS, **64**[e,g]						
mononuclear	⁷Li	5.14	4.3		0.66	8.5
250 K	¹H	5.17	4.3			
dinuclear	⁷Li	4.32	5.3		1.33	9.8
250 K	¹H	4.26	5.3			
HMDS[e,g]	¹H	7.83	2.8	3.2		
250 K						
TMSS	¹H	0.233	4.3	4.4		

[a] All at 60 mM. η(THF, 155 K) = 10.431 × 10⁻³ kg s⁻¹ m⁻¹. η(THF, 250 K) = 0.825 × 10⁻³ kg s⁻¹ m⁻¹. η(THF, 252 K) = 0.801 × 10⁻³ kg s⁻¹ m⁻¹. [b] Experimental error is ca. ±2%. [c] Standard deviation is ca. ±0.1 Å. [d] Estimated using ChemBats3D by averaging the distances between the centroid and the outer hydrogen. [e] A coaxial NMR tube (ID = 1.96 mm; OD = 2.97 mm) separated by a spacer was used. See ref 58. [f] Not obtained. [g] Concentration of 600 mM.

= 6,6′-dimethylbiphenyl-2,2′-diyl) bis(diphenylphosphine), X = BF₄⁻, **65a**, PF₆⁻, **65b,** and CF₃SO₃⁻, **65c,**

65
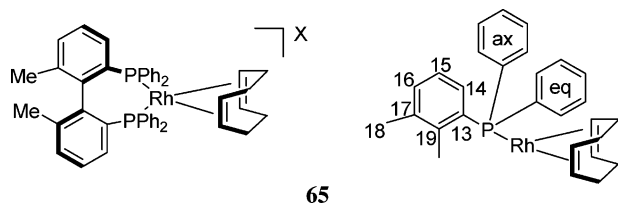
are worth mention in connection with placing the
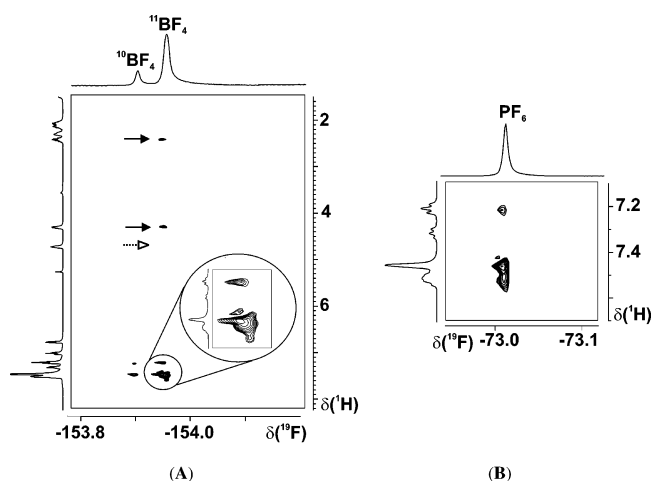
Figure 11. (A) Section of the ¹H,¹⁹F HOESY spectrum[98] for **65a** showing various selective contacts to (a) one of the olefinic protons of the 1,5- COD (bold arrow, δ = 4.37) and not to the other (dashed arrow, δ = 4.72), (b) one aliphatic proton of the 1,5- COD, δ = 2.58, (c) two nonequivalent sets of ortho P-phenyl resonances, δ = 7.21 and δ = 7.46, and (d) a broad signal covering H-14, δ ca. 7.5, from the Biphemp backbone. (B) Section of the ¹⁹F,¹H HOESY spectrum for **65b** showing stronger contacts to the ortho protons of the pseudoequatorial P-phenyl ring and to one proton, H-14, at ca. 7.5 ppm, from the Biphemp backbone. There is a weaker contact to the ortho protons of the pseudoaxial P-phenyl ring and no contact to the olefinic protons. The 7.5 resonance is obscured by overlap with meta protons of the pseudoequatorial P-phenyl ring (CD₂-Cl₂, 400 MHz).

anion in three-dimensional space (see Figure 11 and Table 15).[98] Based on the metal and phosphorus chemical shifts plus the ¹J(Rh, P) values, these three rhodium salts are simply identical. In dichloromethane solution, the observed r_H values are about 6.2 Å for the cations and >4 Å for the anions in all three salts, implying significantly but perhaps not drastically differing amounts of ion pairing. As usual, in CDCl₃, the ion pairing is stronger. The situation changes when one asks about the relative positions of the anions, and for this one resorts to ¹H,¹⁹F HOESY data. Figure 11A shows HOESY data for **65a**, from which an interesting selectivity is observed. We find that the BF₄⁻ anion is close to both of the two

Table 15. D (10^{-10} m² s⁻¹), r_H Values, and Other NMR Parameters (δ in ppm and J in Hz)[a] for the Complexes 65 in CD₂Cl₂ and CDCl₃[98]

	D	r (Å)	δ^a (¹⁰³Rh)	δ^a (³¹P)	¹J (Rh,P)
		65a (X = BF₄)			
cation	8.68	6.2	−109.0	26.3	145
anion	13.38	4.0			
cation[b]	6.14	6.8			
anion[b]	6.41	6.5			
		65b (X = PF₆)			
cation	8.61	6.2	−109.9	26.4	145
anion	12.13	4.4			
cation[b]	6.23	6.7			
anion[b]	5.97	6.9			
		65c (X = CF₃SO₃)			
cation	8.79	6.1	−109.4	26.3	145
anion	12.04	4.4			
cation[b]	6.00	6.9			
anion[b]	5.72	7.2			

[a] 2 mM solutions in CD₂Cl₂. [b] 2 mM CDCl₃.

nonequivalent sets of ortho P-phenyl resonances from the pseudoaxial and pseudoequatorial rings (assigned via a ³¹P,¹H correlation). There are also relatively strong contacts to one Biphemp backbone proton, H-14, and to only one of the two nonequivalent COD-olefinic resonances. Further, there is a contact to a methylene group in the 1,5-COD. This latter resonance corresponds, presumably, to a CH_2 adjacent to the $=CH$ showing the contact. There are no contacts to the Biphemp methyl group. Clearly the BF_4^- anion is choosing a selective pathway (presumably toward the slightly positive P-atoms) and does not drift around the periphery of the cation.

The analogous ¹H,¹⁹F HOESY data for the PF_6^- salt **65b** (Figure 11B) again show contacts to the two nonequivalent sets of ortho P-phenyl resonances (pseudoequatorial stronger than the pseudoaxial P-phenyl ring) and one to H-14 from the Biphemp backbone but no strong contacts to the 1,5-COD ligand. For the triflate, **65c**, there are now generally much weaker contacts. Specifically, the ortho P-phenyl resonances of the pseudoequatorial ring are relatively strong, but there is a much weaker interaction with the pseudoaxial ring and again nothing to the 1,5-COD. Although the immediate coordination sphere of the cation does not sense the change in the anion, the PGSE diffusion and ¹H,¹⁹F HOESY data[19] reveal that, in addition to some ion pairing, each of the anions in **65** demonstrate selectivity in their approach toward the cation.

With respect to the applications of ¹H,¹⁹F HOESY methods to the structures of transition metal salts, Macchioni and co-workers have proven to be the leading research group, and a comprehensive review article on this subject has just appeared.[99b] In a series of papers,[99–109] they have shown that many anions adopt rather specific positions with respect to their cations. Figure 12 shows a nice example based on a [RuCl(diimine)(p-cymene)]BF_4 salt.[90a] The HOESY contacts are not only relatively strong but also quite selective in that the anion lies close to the azabutadiene moiety but remote from the chloride ligand. The combination of PGSE (ion pairing) and HOESY (structure) methodologies provides a potent tool for the discussion on anion effects, which follows.

3. Homogeneous Catalysis

It is well-known that anions can play important roles in a variety of catalytic processes.[83,110–118] The source of these effects is often completely unknown and may be related to coordination or ion pairing effects, among other explanations. Increasingly, ionic liquids are used in catalytic reactions.[119–121] However, exactly how these ions interact with substrate or cosolvent is not well documented.

Empirically, it has been observed that tetraphenyl borate derivatives, and especially the BArF anion,

BArF
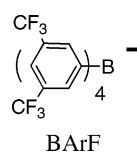
seem to be associated with more efficient catalysts.
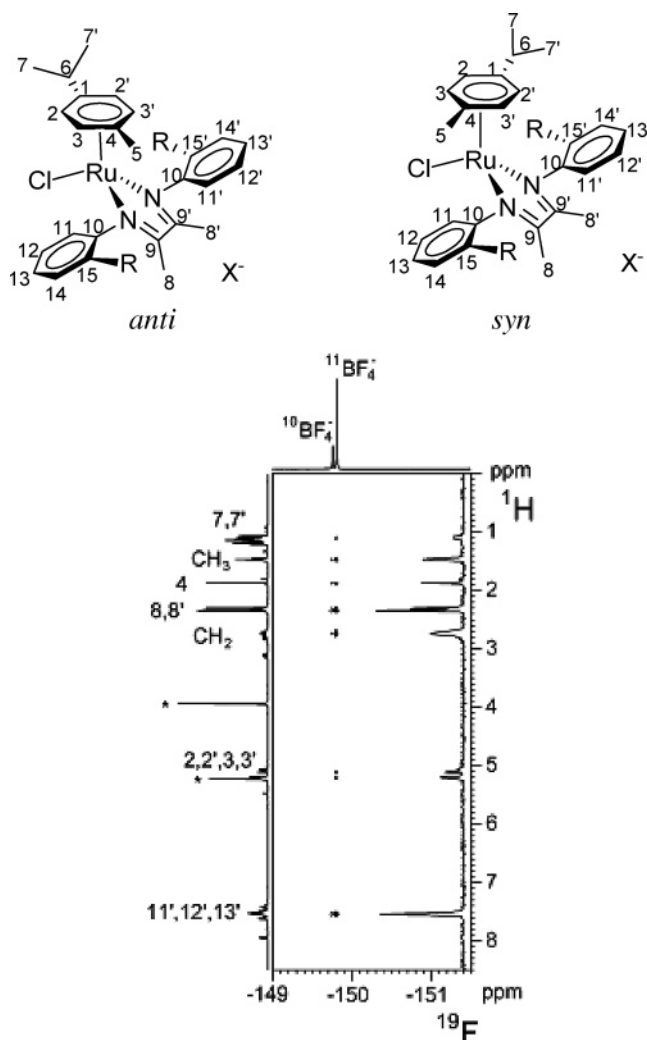
Figure 12. ¹H,¹⁹F HOESY NMR spectrum of [RuCl-(diimine)(p-cymene)]BF_4 *anti* salt.[90a] The F1 trace (indirect dimension) relative to the ¹¹BF_4^- resonance is reported on the right. Asterisks denote the residual nondeuterated resonances of 2-propanol-d_8.

An example of this type of anion dependence is shown in Scheme 9 for the Ru-catalyzed enantioselective Diels−Alder condensation.[116] The choice of the BArF anion results in a significantly faster (but not more enantioselective) process. The observed rates decreased in the order $BArF^- > SbF_6^- > PF_6^- > BF_4^-$.

The PGSE/HOESY approach seemed likely to shed some light on this anion dependence.[83] Consequently, several sets of model complexes were prepared and studied, and the PGSE data from these are given in Tables 16−18. The model complexes chosen contain BINAP (as model for a large chiral bidentate phosphine donor), Tables 16 and 17, and then BIPHOP, Table 18. The measured D-values for [RuCl(η^6-p-cymene)(BINAP)]⁺, **66**, and [Ru(η^5−C_5H_5)(BINAP)-(CH_3CN)]⁺, **67**, in several solvents provide the necessary background data so that the results from the acrylonitrile BIPHOP models for the catalyst precursors, [Ru(η^5−C_5H_5)(CH_2=CHCN)(BIPHOP−F)][Y], **68,** and [Ru(η^5−C_9H_7)(CH_2=CHCN)(BIPHOP−F)][Y], **69**, will be more readily interpreted.

As we have now come to expect, the chloroform data from Tables 16 and 17 reveal tight ion pairing,

Scheme 9

Y = BF$_4$, SbF$_6$, BArF   (R,R)-BIPHOP-F

exo
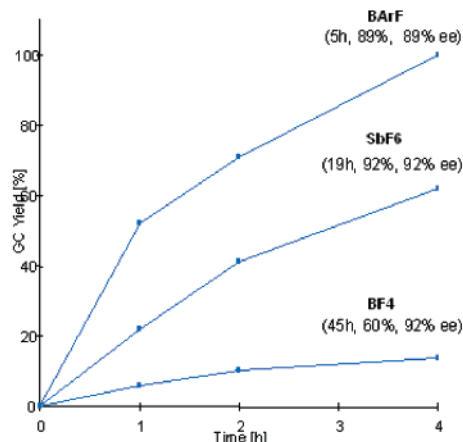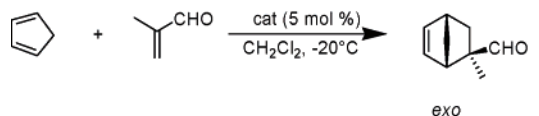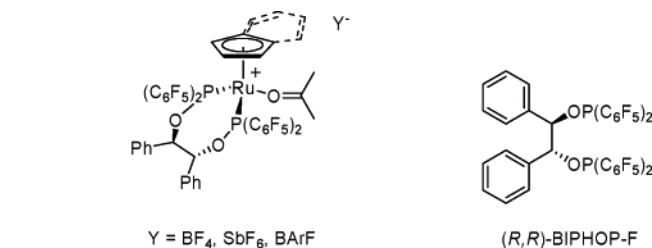
Table 16. D (10^{-10} m^2 s^{-1}) and r_H (Å) values for **66a–f**[a] in CD$_3$OD, CD$_2$Cl$_2$, CDCl$_3$, and (CD$_3$)$_2$CO

66a: X = BF$_4$
66b: X = OTf
66c: X = BArF
66d: X = PF$_6$

compd	fragment	CD$_3$OD		CD$_2$Cl$_2$		CDCl$_3$		(CD$_3$)$_2$CO	
		D^b	$r_H{}^c$	D^b	$r_H{}^c$	D^b	$r_H{}^c$	D^b	$r_H{}^c$
66a BF$_4$	cation (^{1}H)	5.98	7.0	7.89	6.8	5.89	7.0	10.07	7.2
	anion (^{19}F)	15.73	2.6	10.95	4.9	5.99	6.9	26.85	2.7
66b OTf	cation (^{1}H)	5.96	7.0	7.73	6.9	5.93	7.0	9.95	7.3
	anion (^{19}F)	12.28	3.4	10.46	5.1	6.05	6.9	23.39	3.1
66c BArF	cation (^{1}H)	5.98	7.0	7.71	6.9	4.78	8.6	9.91	7.3
	anion (^{19}F)	6.42	6.5	8.05	6.6	4.88	8.5	10.83	6.7
NaBArF	anion (^{19}F)	6.53	6.3						
66d PF$_6$	cation (^{1}H)			7.87	6.8				
	anion (^{19}F)			10.99	4.9				

^{a} 2 mM. ^{b} Estimated using the diffusion coefficient of HDO in D$_2$O as ref 81. Standard deviation is ca. 0.1. ^{c} η (300 K, kg s^{-1} m^{-1}): CH$_3$OH = 0.526; CH$_2$Cl$_2$ = 0.410; CHCl$_3$ = 0.529; (CH$_3$)$_2$CO = 0.303.

that is, close to equivalent translation rates for both cation and anion, and the calculated r_H values are larger in chloroform than, for example, dichloromethane, especially for the BArF$^-$ salt. Note that in acetone, the BF$_4{}^-$, CF$_3$SO$_3{}^-$, and PF$_6{}^-$ all give relatively small r_H values, ca. 2.7–2.9 Å. These values are similar to those found for a variety of BF$_4{}^-$ salts in methanol solution.

In dichloromethane solutions of **66** and **67**, the r_H values for the BF$_4{}^-$, CF$_3$SO$_3{}^-$, and PF$_6{}^-$ anions are all relatively large and suggest a significant amount

Table 17. Diffusion Values (10^{-10} m^2 s^{-1})^a and Hydrodynamic Radii (Å) for 67a–d

67a: Y = BF$_4$
67b: Y = CF$_3$SO$_3$
67c: Y = PF$_6$
67d: Y = BArF

BINAP

compd	fragment	CD$_2$Cl$_2$		CDCl$_3$		(CD$_3$)$_2$CO	
		D	r_H	D	r_H	D	r_H
67a BF$_4$	cation (^{1}H)	8.26	6.5	6.07	6.8	10.73	6.8
	anion (^{19}F)	12.33	4.3	6.14	6.8	26.84	2.7
67b CF$_3$SO$_3$	cation (^{1}H)	8.16	6.6	6.00	6.9	10.51	6.9
	anion (^{19}F)	12.16	4.4	6.14	6.8	24.63	2.9
67c PF$_6$	cation (^{1}H)	8.36	6.4	6.13	6.8	10.64	6.8
	anion (^{19}F)	12.30	4.4	6.52	6.4	26.89	2.7
67d BArF	cation (^{1}H)	7.76	6.9	4.78	8.6	10.31	7.0
	anion (^{1}H)	7.93	6.8	4.97	8.5	11.47	6.3
	neutral (^{1}H)	8.51	6.3	6.53	6.4		

^{a} 2 mM.

Table 18. Diffusion Values (10^{-10} m^2 s^{-1}) and Hydrodynamic Radii (Å) for 68a,b and 69a,b^a

RR-68a : η^5-C$_5$H$_5$; **L** : Acrylonitrile ; Y = BF$_4$
RR-68b : η^5-C$_5$H$_5$; **L** : Acrylonitrile ; Y = BArF
69a : η^5-C$_9$H$_7$; **L** : Acrylonitrile ; Y = BF$_4$
69b : η^5-C$_9$H$_7$; **L** : Acrylonitrile ; Y = BArF

compd	fragment	CD$_2$Cl$_2$		(CD$_3$)$_2$CO	
		D	r_H	D	r_H
(R,R)-**68a** BF$_4$	cation (^{1}H)	7.84	6.8	9.72	7.5
	anion (^{19}F)	9.67	5.5	27.36	2.6
(R,R)-**68b** BArF	cation (^{1}H)	7.28	7.4	9.44	7.7
	anion (^{1}H)	7.84	6.8	11.85	6.1
69a BF$_4$	cation (^{1}H)	7.80	6.9	9.17	7.9
	anion (^{19}F)	9.79	5.5	24.45	3.0
69b BArF	cation (^{1}H)	7.20	7.4	9.16	7.9
	anion (^{1}H)	7.90	6.8	11.44	6.3

^{a} 2 mM.

of ion pairing. ^{1}H,^{19}F HOESY spectra measured in dichloromethane support this conclusion.

With this background, we turned our attention to the BIPHOP–F complexes, **68** and **69**.[122] In methylene chloride solution (the solvent used in the catalytic chemistry), the calculated r_H values (5.5 Å) for the BF$_4{}^-$ anion in both (R,R)-**68a** and **69a** are clearly too large to arise from a simple solvate of BF$_4{}^-$ and suggest relatively strong ion pairing. The 5.5 Å value was the largest r_H that we have yet found for this anion in this solvent. However, the cation r_H values, ca. 6.8–6.9 Å, are reasonable enough.

For the BArF salts, in dichloromethane solution **68b** and **69b** both afford r_H values for the cation of ca. 6.8 Å. A typical r_H value for BArF salts in acetone or methanol is ca. 6.1–6.3 Å; therefore, a 6.8 Å value is consistent with some interactions but would not be considered as a predominant ion pairing.

To further explore the observed solvent dependence of the ion pairing, the ^{1}H,^{19}F HOESY spectra for these complexes were measured. These spectra show selective contacts to one of the CHO backbone signals, the vinyl protons of the acrylonitrile, and the η^5-ligand and additional contacts to the ortho protons of one of the phenyl groups (see Figure 13). There
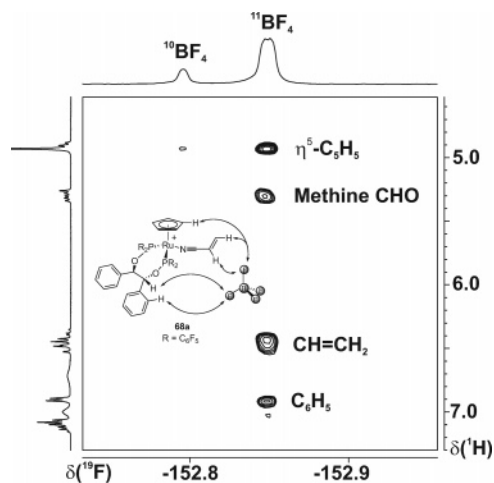
Figure 13. The ^{1}H,^{19}F HOESY spectrum of complex [Ru($\eta^5-C_5H_5$)(CH$_2$=CHCN)(BIPHOP−F)][BF$_4$], **68a**.[83] Note that only one of the CHO backbone resonances, at ca. 5.3 ppm, shows a cross-peak and that there is selectivity to one of the phenyl rings. The second methine CHO signal appears to low frequency of the η^5-C$_5$H$_5$ resonance.

are no HOESY contacts from the BArF to the cation.

If the BF$_4^-$ anion ion pairs strongly, it might well interfere with the complexation of the dienophile oxygen donor or decrease the rate of aldehyde (product) exchange once the condensation has occurred. Either of the above would be sufficient to slow the reaction. Kinetic studies suggest that the Diels−Alder condensation is not rate-determining.[83] The BArF$^-$ anion is not so strongly ion paired, and HOESY data (and X-ray data,[83] not discussed here) reveal little or no contacts between the CF$_3$ groups (or ortho aryl protons) and the cation. The increased distance of this anion from the reactive site would provide a rational for the higher turn-over frequency of the catalyst.

Chiral oxazoline complexes of the late transition metals are recognized[123−128] as successful enantioselective catalysts in an increasing number of organic transformations. Specifically, the Ir(I) catalyst precursor Ir(1,5-COD)(**70**)](BArF), **71a**, has

R^1 = CH$_3$, R^2 = t-butyl

70
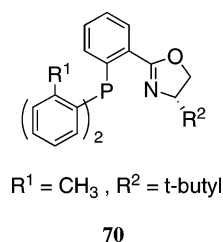
been shown to hydrogenate trisubstituted olefins in methylene chloride with excellent enantioselectivity (see eq 3).[128]

ee = 98%
yield = 99%
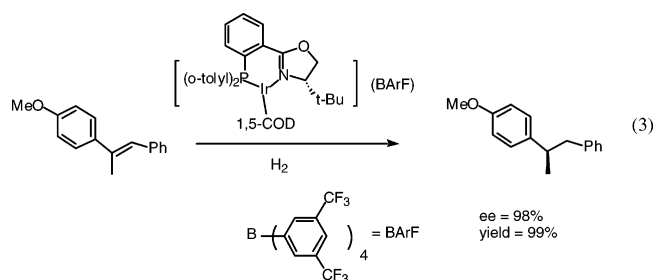
There are relatively few homogeneous catalysts capable of efficiently reducing tri- and tetra-substituted olefins.[129] However, the lifetime and the activity of the catalyst in eq 3 have been shown to depend on the nature of the anion, with the PF$_6^-$ derivative having a rather shorter lifetime than the analogous BArF$^-$ derivative, see Figure 14.[128a] It is tempting to think that, in analogy with **68** and **69**, the ion pairing will prove to be the source of this dependence; however, as we will show, this conclusion is not completely correct.

In contrast to the Diels−Alder chemistry described above, complex **71** undergoes a major transformation before it can function in the hydrogenation chemistry. Molecular hydrogen is oxidatively added to form a dihydride species, which then reduces the diolefin to cyclooctane. A new dihydride−olefin (substrate) complex is generated, which, after migratory insertion and reductive elimination steps, eventually leads to an Ir(I) species, which then re-enters the catalytic cycle via reaction with H$_2$. Consequently, there are a number of intermediates to study, many of which are not very stable, so the choice of the most relevant model complex is not immediately obvious. We have prepared several iridium dihydride complexes of the form [IrH$_2$(**70**)(L1)(L2)](anion), **72**,[129a] where the two
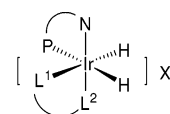
72a = PF$_6$ or **72b**, =BArF   P,N = **70**
L1L2 = 4,4'-dimethylpyridine

L ligands can be either monodentate donors or a single bidentate donor, for example, 4,4′-dimethylpyridine. Moreover, in the study of the various dihydride complexes in the catalytic solution, we noted that a trinuclear hydrido cluster, **73**, was formed.[129b−c]

[Ir(1,5-COD)(**P-N**)]X

71b X = PF$_6$
71c X = OTf

[Ir$_3$(μ^3-H) (H)$_6$(**P-N**)$_3$]X$_1$X$_2$

73a X$_1$ = PF$_6$ X$_2$ = OTf
73b X$_1$ = X$_2$ = PF$_6$
73c X$_1$ = X$_2$ = OTf   (4)
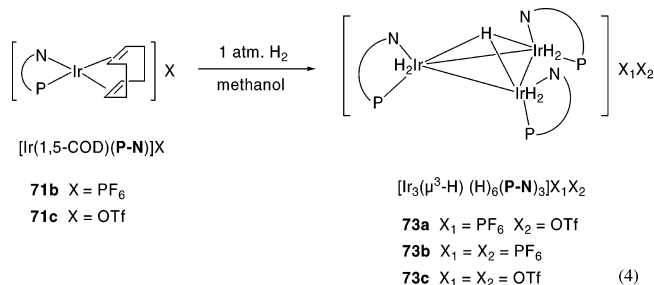
The hint came from a ^{31}P,^{1}H correlation spectrum, see Figure 15, in which an unexpected quartet multiplicity was observed.
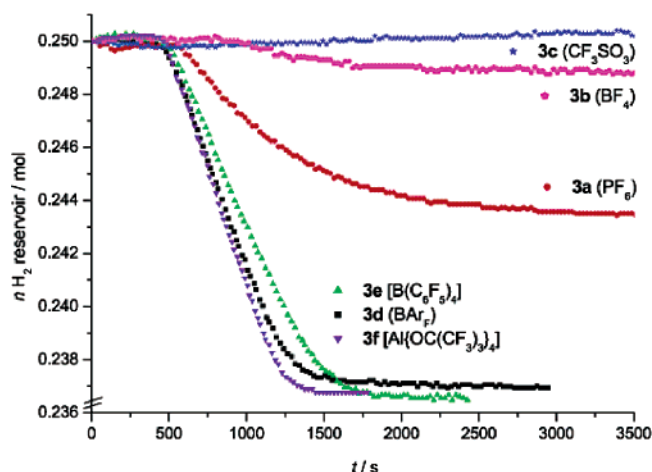
Figure 14. Hydrogen consumption for catalytic reactions with 0.1 mol % of Ir(I) complex **71** with different anions at 14 bar of H_2, 4 °C, stirring speed 1200 min^{-1}.[128a]
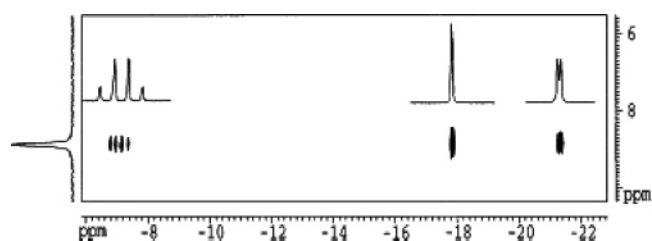
Figure 15. Section of ^{31}P,^1H correlation for **73** showing the three hydride ligands, where one of the signals shows an unexpected spin multiplicity.[129b] The quartet multiplicity comes from three equivalent ^{31}P spins.

Eventually, several of these could be prepared in high yield by reaction of **71b,c** with hydrogen in methanol solution (see eq 4). A brief search of the literature revealed that Crabtree and co-workers[130] and Pignolet and co-workers[131] had reported this type of iridium cluster earlier. These clusters were thought *not to be catalytically active* in hydrogenation chemistry and indeed **73** is *not* a hydrogenaton catalyst.

Diffusion data for these three classes, **71**−**73**, are shown in Tables 19−21. Before discussing these data, it is important to emphasize that the anion effect presumably involves the change in kinetics for a deactivation process, that is, one or more of the anions under consideration prohibits the formation of the cluster long enough to allow the hydrogenation to go to completion. In our hands, all of the anions eventually produce some cluster.

Although the *D*-values shown in Tables 19−21 will prove useful as reference data, the important conclusions for the dichloromethane solutions are as follows: (a) For **71**, there is some but not an unusual amount of ion pairing. Put differently, there is no reason to assume that the smaller anions interfere with either complexation or decomplexation. (b) For the few examples shown for **72**, there seems to be a somewhat larger degree of ion pairing in the BArF analogue. (c) For **73**, there seems to be more ion pairing, but this is presumably not important because this cluster is catalytically inactive.

In general, one finds modest-to-strong HOESY contacts for the smaller anions but weak to nonobservable contacts from BArF. The absence of strong

Table 19. Diffusion Values (10^{-10} m^2 s^{-1}),[a] Hydrodynamic Radii (Å) and Volumes ($\times10^2$, Å^3) for 71

	CD$_3$OD			CDCl$_3$		
	D	r_H	*V*	*D*	r_H	*V*
71a BF$_4$						
cation (^1H)	7.58(6)	5.5(1)	7.0	7.23(6)	5.7(1)	7.7
anion (^{19}F)	16.62(6)	2.5(1)	0.6	7.43(6)	5.6(1)	7.4
71b PF$_6$						
cation (^1H)	7.57(6)	5.5(1)	7.0	7.13(6)	5.8(1)	8.2
anion (^{19}F)	15.82(6)	2.6(1)	0.7	7.21(6)	5.8(1)	8.2
71c OTf						
cation (^1H)	7.65(6)	5.5(1)	7.0	7.04(6)	5.9(1)	8.6
anion (^{19}F)	12.95(6)	3.2(1)	1.4	7.05(6)	5.9(1)	8.6
71d B(C$_6$F$_5$)$_4$						
cation (^1H)	7.62(6)	5.5(1)	7.0	6.06(6)	6.9(1)	14
anion (^{19}F)	7.69(6)	5.4(1)	6.6	5.91(6)	7.0(1)	14
71e BArF						
cation (^1H)	7.55(6)	5.5(1)	7.0	5.70(6)	7.3(1)	16
anion (^1H)	6.77(6)	6.2(1)	10	5.63(6)	7.4(1)	17
anion (^{19}F)	6.67(6)	6.2(1)	10	5.59(6)	7.4(1)	17

	CD$_2$Cl$_2$			ClCH$_2$CH$_2$Cl		
	D	r_H	*V*	*D*	r_H	*V*
71a BF$_4$						
cation (^1H)	9.72(6)	5.5(1)	7.0	5.44(6)	5.4(1)	6.6
anion (^{19}F)	13.79(6)	3.9(1)	2.5	8.52(6)	3.4(1)	1.6
71b PF$_6$						
cation (^1H)	9.72(6)	5.5(1)	7.0	5.37(6)	5.4(1)	6.6
anion (^{19}F)	13.27(6)	4.0(1)	2.7	8.00(6)	3.6(1)	1.9
71c OTf						
cation (^1H)	9.71(6)	5.5(1)	7.0	5.36(6)	5.4(1)	6.6
anion (^{19}F)	12.52(6)	4.3(1)	3.3	7.67(6)	3.8(1)	2.3
71d B(C$_6$F$_5$)$_4$						
cation (^1H)	9.24(6)	5.8(1)	8.2	5.17(6)	5.7(1)	7.7
anion (^{19}F)	9.12(6)	5.9(1)	8.6	5.08(6)	5.8(1)	8.2
71e BArF						
cation (^1H)	9.20(6)	5.8(1)	8.2	5.09(6)	5.7(1)	7.7
anion (^1H)	8.40(6)	6.4(1)	11			
anion (^{19}F)	8.43(6)	6.4(1)	11	4.71(6)	6.2(1)	10

^{a} At 2 mM.

HOESY contacts in the BArF analogues is ambiguous in that the anion cannot be very far away because we observe some ion pairing.

Clearly, we cannot directly extrapolate our diffusion data to catalytic solutions because we have not measured materials whose structures strongly correlate to the catalytic structures in solution. However, if the mechanism of the formation of an inactive Ir$_3$ cluster requires that two fairly large species associate and subsequently add yet another large moiety, then in methylene chloride, these processes are likely to be faster for a salt containing a relatively small rapidly moving anion, such as PF$_6^-$, than for a larger, partially ion-paired complex with, for example, BArF$^-$. Most likely, a combination of steric effects (i.e., the BArF is large enough to make it difficult for a second iridium moiety to approach) and ion pairing (the anion is never far away) contribute to making the larger anions less likely to form the inactive cluster.

The use of metallocene complexes as single site polymerization catalysts remains an area of intense research.[117a] The nature of the counterion is recog-

Table 20. Diffusion Data (10^{-10} m^2 s^{-1}),^{a} Hydrodynamic Radii (Å), and Volumes ($\times10^2$, Å^3) for the Trinuclear Hydride Compound 73

	CD$_3$OD			CDCl$_3$		
	D	r_H	V	D	r_H	V
73a (PF$_6$)(OTf)^b						
cation (^{1}H)	5.09(6)	8.2(1)	23	4.64(6)	8.9(1)	29
PF$_6$ (^{19}F)	15.16(6)	2.7(1)	0.8	4.70(6)	8.8(1)	29
OTf (^{19}F)	12.34(6)	3.4(1)	1.6	4.71(6)	8.8(1)	29
73b (PF$_6$)$_2$^{b}						
cation (^{1}H)	5.06(6)	8.2(1)	23	4.94(6)	8.4(1)	25
PF$_6$ (^{19}F)	15.51(6)	2.7(1)	0.8	5.12(6)	8.1(1)	22
73c (OTf)$_2$						
cation (^{1}H)	5.10(6)	8.2(1)	23	4.33(6)	9.6(1)	37
OTf (^{19}F)	12.12(6)	3.4(1)	1.6	4.43(6)	9.4(1)	35

|	CD$_2$Cl$_2$			ClCH$_2$CH$_2$Cl		
	D	r_H	V	D	r_H	V
73a (PF$_6$)(OTf)						
cation (^{1}H)	6.43(6)	8.3(1)	24	3.50(6)	8.3(1)	24
PF$_6$ (^{19}F)	9.65(6)	5.5(1)	7.0	6.04(6)	4.8(1)	4.6
OTf (^{19}F)	9.82(6)	5.5(1)	7.0	6.19(6)	4.7(1)	4.3
73b (PF$_6$)$_2$						
cation (^{1}H)	6.53(6)	8.2(1)	23	3.57(6)	8.2(1)	23
PF$_6$ (^{19}F)	9.57(6)	5.6(1)	7.3	6.21(6)	4.7(1)	4.3
73c (OTf)$_2$						
cation (^{1}H)	6.47(6)	8.3(1)	24	3.52(6)	8.3(1)	24
OTf (^{19}F)	9.84(6)	5.4(1)	6.6	5.83(6)	5.0(1)	5.2

^{a} At 2 mM. ^{b} Saturated solution (less than 2 mM).

Table 21. Selected Diffusion Data (10^{-10} m^2 s^{-1}),^{a} Hydrodynamic Radii (Å), and Volumes ($\times10^2$, Å^3) for the Dihydride Compounds 72a and 72b in CD$_2$Cl$_2$

	72a PF$_6$			72b BArF		
	D	r_H	V	D	r_H	V
cation (^{1}H)	9.09(6)	5.9(1)	8.6	8.09(6)	6.6(1)	12
anion (^{19}F)	13.65(6)	3.9(1)	2.5	7.93(6)	6.8(1)	13

^{a} At 2 mM.

nized to be an essential component with respect to both structure and reactivity. For example, in the active species of a cationic zirconocene-based catalyst, ion pairing is thought to be important in this chemistry. The cations may be generated from metallocene dichlorides using MAO (methylaluminoxane)[132] or from dialkyl complexes using B(C$_6$F$_5$)$_3$ or related reagents,[117,132] and much effort (including many NMR studies[133]) has been expended toward understanding the chemistry of these catalysts.

Early on, Brintzinger and co-workers[134b] suggested an anion-exchange process via ion quadrupoles and supported their views via PGSE studies. Moreover, in a recent study involving the reaction system Zr(Me)$_2$(Cp)$_2$/MAO, Babushkin and Brintzinger have estimated the size of the ion pair, **74**, by PGSE

74
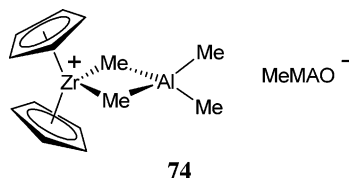
methods.[134a] A mean effective hydrodynamic radius

of 12.2−12.5 Å was determined from the D-values in benzene solution at different zirconocene and MAO concentrations. At elevated concentrations, aggregation to ion quadrupoles or higher aggregates is thought to occur.

This question of aggregation seems strongly linked to the concentration under study. Stahl et al.,[135] in their investigation of several zirconocene salts using PGSE and cryoscopic methods, have found "no evidence of significant aggregation at concentrations in the 1−18 mM regime." This brings us back to the useful study by Zuccaccia et al.[66] on their various ziconocene salts and the data in Tables 10 and 11. The D-values (from Table 11) for the complex salt [Zr(Me)(THF)(Me$_2$SiCp)$_2$](MeB(C$_6$F$_5$)$_3$), **75**, in the range 0.09−2.20 mM change from 6.74×10^{-10} to 5.17×10^{-10} m^2 s^{-1}. This concentration range results in a relatively large change in the hydrodynamic radius, from 5.2 Å for the dilute solution up to 6.2 Å for the more concentrated solution, and these are not very concentrated solutions.

Diffusion data in 2-propanol solution for the catalyst precursor **76** as a function of concentration have

76
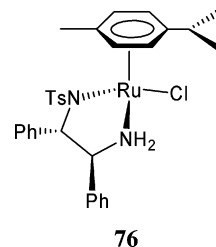
recently been reported by Macchioni and co-workers[90c] (see Table 22). An approximate factor of 80 change

Table 22. Diffusion Coefficients (10^{-10} m^2 s^{-1}), Hydrodynamic Radii (r_H, Å), c Factors, Hydrodynamic Volumes (V_H, Å^3), and Aggregation Numbers (N) as a Function of Concentration (C, mM) in Isopropanol-d_8 (Unless Noted Otherwise) for 76

entry	D	r_H	c	V_H	N	C
1	1.6	5.8	5.2	833	1.8	0.05
2	1.6	5.8	5.2	842	1.8	0.2
3	1.6	6.2	5.2	988	2.1	1.0
4	1.5	6.3	5.3	1051	2.3	4.0
5	1.4	6.7	5.4	1264	2.8	12.0
6	1.1	7.6	5.5	1823	4.0	42.0^a
7^b	6.1	6.4	5.5	1087	2.4	2.0
8^b	4.6	8.1	5.7	2242	4.9	12.0
9^c	11.4	5.8	5.3	815	1.8	2.0
10^d	6.3	5.8	5.5	834	1.8	2.0
11^e	1.6	6.6	5.5	1204	2.6	2.0

^{a} Saturated solution. ^{b} In CDCl$_3$. ^{c} In acetone-d_6. ^{d} In methanol-d_4. ^{e} In DMSO-d_6.

in concentration produces a ca. 50% change in the observed D-value with the result that the hydrodynamic radius changes from 5.8 to 7.6 Å. Clearly, a correct interpretation of the PGSE data from materials such as **75** or **76** will require a series of measurements combined with the appropriate Overhauser and (additional) support studies.

4. Conclusions

It is interesting that this ca. 40 year old NMR methodology has, at least from the point of view of

the inorganic/organometallic chemist, been rejuvenated. Apart from the "classical" use of PGSE measurements (or the more recent DOSY variant), as a tool to estimate molecular volumes, it would appear that diffusion data provide a unique, relatively rapid way of recognizing and evaluating the general problem of ion pairing. This is a relatively new application and often requires a multinuclear approach. However, when combined with Overhauser data (be they from HOESY or NOESY spectra), these methods allow us to consider problems and explain observations that would otherwise remain puzzling simply because we lack the necessary tools. The observed anion effect in selected homogeneously catalyzed reactions represents a nice example of this type of application.

With the use of these NMR methods, the anion is no longer a nondescript "X", because one can now prove whether it is or is not involved in specific interactions with the cation and, moreover, where it sits. The PGSE methodology is (in the opinion of the present authors) semiquantitative, so explanations of various chemical phenomena attributed to "ion pairing" can be readily tested in that one can easily estimate the extent of the ion pairing. It is also becoming clear that certain solvents promote strong ion pairing (e.g., chloroform) and that the use of low temperatures may influence how ions interact. Fortunately, NMR spectrometer sensitivity continues to improve. Consequently, measuring at realistic concentrations (i.e., less than 1 mM) is no longer just a dream, and thus one can hope to avoid the problems associated with aggregation induced by relatively high concentrations. However, for diffusion measurements on nuclei such as ^{7}Li or ^{195}Pt, this problem still exists.

Of course any molecular interactions that affect translation, for example, hydrogen bonding and host−guest encapsulation, can also be monitored via PGSE methods, and the published applications of diffusion methods in these research areas continue to grow. However, given the importance of ionic interactions in the various branches of chemistry, it seems likely that the applications of PGSE and related diffusion methodologies will expand strongly in this direction.

5. Acknowledgments

6. References

(1) Stejskal, E. O.; Tanner, J. E. *J. Chem. Phys.* **1965**, *42*, 288.
(2) (a) Johnson, C. S. J. *Prog. NMR Spectrosc.* **1999**, *34*, 203. (b) Johnson, C. S. J. In *Encyclopedia of Nuclear Magnetic Resonance*; Grant, D. M., Harris, R. K., Eds.; Wiley: Chichester, U.K., 1996; p 1626.
(3) (a) Price, W. S. *Ann. Rep. NMR Spectrosc.* **1996**, *32*, 51. (b) Price, W. S. *Concepts Magn. Reson.* **1997**, *9*, 299. (c) Price, W. S. *Concepts Magn. Reson.* **1998**, *10*, 197.
(4) (a) Stilbs, P. *Prog. NMR Spectrosc.* **1987**, *19*, 1. (b) Antalek, B. *Concepts Magn. Reson.* **2002**, *14*, 225. (c) Lucas, L. H.; Larive, C. K.; *Concepts Magn. Reson.* **2004**, *20A*, 24.
(5) Fichele, S.; Paley, M. N. J.; Woodhouse, N.; Griffiths, P. D.; van Beek, E. J. R.; Wild, J. M. *J. Magn. Reson.* **2004**, *167*, 1.
(6) Fichele, S.; Paley, M. N. J.; Woodhouse, N.; Griffiths, P. D.; van Beek, E. J. R.; Wild, J. M. *Magn. Reson. Med.* **2004**, *52*, 917.
(7) Kuchel, P. W.; Eykyn, T. R.; Regan, D. G. *Magn. Reson. Med.* **2004**, *52*, 907.
(8) (a) Wan, Y.; Angleson, J. K.; Kutateladze, A. G. *J Am. Chem. Soc.* **2002**, *124*, 5610. (b) Yan, J. L.; Kline, A. D.; Mo, H. P.; Zartler, E. R.; Shapiro, M. J. *J. Am. Chem. Soc.* **2002**, *124*, 9984. (c) Kaucher, M. S.; Lam, Y.-F.; Pieraccini, S.; Gottarelli, G. A.; Davis, J. T. *Chem.−Eur. J.* **2005**, *11*, 164.
(9) Hayamizu, K.; Akiba, E.; Bando, T.; Aihara, Y.; Price, W. S. *Macromolecules* **2003**, *36*, 2785.
(10) Hayamizu, K.; Aihara, Y.; Price, W. S. *J. Chem. Phys.* **2000**, *113*, 4785.
(11) Griffiths, P.; Stilbs, P. *Curr. Opin. Colloid Interface Sci.* **2002**, *7*, 249.
(12) (a) Balinov, B.; Linse, P.; Soderman, O. *J. Colloid Interface Sci.* **1996**, *182*, 539. (b) Soderman, O.; Balinov, B. *Surfactant Sci. Ser.* **1996**, *61*, 369. (c) Valentini, M.; Vaccaro, A.; Rehor, A.; Napoli, A.; Hubbell, J. A.; Tirelli, N. *J. Am. Chem. Soc.* **2004**, *126*, 2142. (d) Johannessen, E.; Walderhaug, H.; Balinov, B. *Langmuir* **2004**, *20*, 336.
(13) Gaede, H. C.; Gawrisch, K. *Magn. Reson. Chem.* **2004**, *42*, 115.
(14) Braun, M.; Hartnagel, U.; Ravanelli, E.; Schade, B.; Bottcher, C.; Vostrowsky, O.; Hirsch, A. *Eur. J. Org. Chem.* **2004**, *9*, 1983.
(15) Ihm, H.; Ahn, J. S.; Lah, M. S.; Ko, Y. H.; Paek, K. *Org. Lett.* **2004**, *6*, 3893.
(16) Deaton, K. R.; Feyen, E. A.; Nkulabi, H. J.; Morris, K. F. *Magn. Reson. Chem.* **2001**, *39*, 276.
(17) Kadi, M.; Dvinskikh, S. V.; Furo, I.; Almgren, M. *Langmuir* **2002**, *18*, 5015.
(18) Ludwig, M.; Kadyrov, R.; Fiedler, H.; Haage, K.; Selke, R. *Chem.−Eur. J.* **2001**, *7*, 3298.
(19) (a) Mo, H. P.; Pochapsky, T. C. *J. Phys. Chem. B* **1997**, *101*, 4485. (b) Mo, H. P.; Wang, A. P.; Stone, P.; Wilkinson, S.; Pochapsky, T. C. *J. Am. Chem. Soc.* **1997**, *119*, 11666. (c) Mo, H. P.; Pochapsky, T. C. *Prog. Nucl. Magn. Reson. Spectrosc.* **1997**, *30*, 1. (d) Hoffstetter, C.; Wilkinson, S.; Pochapsky, T. C. *J. Org. Chem.* **1999**, *64*, 8794. (e) Hoffstetter, C.; Pochapsky, T. C. *Magn. Reson.* **2000**, *38*, 90.
(20) (a) Ribot, F.; Escax, V.; Martins, J. C.; Biesemans, M.; Ghys, L.; Verbruggen, I.; Willem, R. *Chem.−Eur. J.* **2004**, *10*, 1747. (b) Ribot, F.; Escax, V.; Roiland, C.; Sanchez, C.; Martins, J. C.; Biesemans, M.; Verbruggen, I.; Willem, R. *Chem. Commun.* **2005**, 1019.
(21) Reger, D. L.; Gardinier, J. R.; Pellechia, P. J.; Smith, M. D.; Brown, K. J. *Inorg. Chem.* **2003**, *42*, 7635.
(22) (a) Schlorer, N. E.; Cabrita, E. J.; Berger, S. *Angew. Chem., Int. Ed.* **2002**, *41*, 107−109. (b) Liger-Belair, G.; Prost, E.; Parmentier, P.; Jeandet, P.; Nuzillard, J. M. *J. Agric. Food. Chem.* **2003**, *51*, 7560.
(23) Aihara, Y.; Bando, T.; Nakagawa, H.; Yoshida, H.; Hayamizu, K.; Akiba, E.; Price, W. S. *J. Electrochem. Soc.* **2004**, *151*, A119.
(24) (a) Jaing, Q.; Rüegger, H.; Venanzi, L. M. *Inorg. Chim Acta* **1999**, *290*, 64. (b) Macchioni, A.; Bellachioma, G.; Cardaci, G.; Gramlich, V.; Ruegger, H.; Terenzi, S.; Venanzi, L. M. *Organometallics* **1997**, *16*, 2139.
(25) Stoop, R. M.; Bachmann, S.; Valentini, M.; Mezzetti, A. *Organometallics* **2000**, *19*, 4117.
(26) Burini, A.; Fackler, J. P.; Galassi, R.; Macchioni, A.; Omary, M. A.; Rawashdeh-Omary, M. A.; Pietroni, B. R.; Sabatini, S.; Zuccaccia, C. *J. Am. Chem. Soc.* **2002**, *124*, 4570.
(27) Cifelli, M.; McDonald, P. J.; Veracini, C. A. *Phys. Chem. Chem. Phys.* **2004**, *6*, 4701.
(28) Kadi, M.; Dvinskikh, S. V.; Furo, I.; Almgren, M. *Langmuir* **2002**, *18*, 5015.
(29) Accardo, A.; Tesauro, D.; Roscigno, P.; Gianolio, E.; Paduano, L.; D'Errico, G.; Pedone, C.; Morelli, G. *J. Am. Chem. Soc.* **2004**, *126*, 3097.
(30) Hayamizu, K.; Price, W. S. *J. Magn. Reson.* **2004**, *167*, 328.
(31) Momot, K. I.; Kuchel, P. W. *J. Magn. Reson.* **2004**, *169*, 92.
(32) Simorellis, A. K.; Flynn, P. F. *J. Magn. Reson.* **2004**, *170*, 322.
(33) Price, W. S.; Hayamizu, K.; Ide, H.; Arata, Y. *J. Magn. Reson.* **1999**, *139*, 205.
(34) Dvinskikh, S. V.; Furo, I.; Sandstrom, D.; Maliniak, A.; Zimmermann, H. *J. Magn. Reson.* **2001**, *153*, 83.
(35) Keresztes, I.; Williard, P. G. *J. Am. Chem. Soc.* **2000**, *122*, 10228.
(36) (a) Cabrita, E. J.; Berger, S. *Magn. Reson. Chem.* **2002**, *40*, S122. (b) Cabrita, E. J.; Berger, S. *Magn. Reson. Chem.* **2001**, *39*, S142.

(37) Cabrita, E. J.; Berger, S.; Brauer, P.; Karger, J. *J. Magn. Reson.* **2002**, *157*, 124.
(38) (a) Johnson, C. S., Jr. *Prog. NMR Spectrosc.* **1999**, *34*, 203. (b) Pelta, M. D.; Barjat, H.; Morris, G. A.; Davis, A. L.; Hammond, S. J. *Magn. Reson. Chem*. **1999**, *36*, 706.
(39) Harris, R. K.; Kinnear, K. A.; Morris, G. A.; Stchedroff, M. J.; Samadi-Maybadi, A. *Chem. Commun.* **2001**, 2422.
(40) Zhao, T.; Beckham, H. W. *Macromolecules* **2003**, *36*, 9859.
(41) Zhao, T.; Beckham, H. W.; Gibson, H. W. *Macromolecules* **2003**, *36*, 4833.
(42) Gambs, C.; Dickerson, T. J.; Mahajan, S.; Pasternack, L. B.; Janda, K. D. *J. Org. Chem.* **2003**, *68*, 3673.
(43) Viel, S.; Capitani, D.; Mannina, L.; Segre, A. *Biomacromolecules* **2003**, *4*, 1843.
(44) Diaz, M. D.; Berger, S. *Carbohydr. Res.* **2000**, *329*, 1.
(45) Hinton, D. P.; Johnson, C. S. *J. Phys. Chem*. **1993**, *97*, 9064.
(46) Viel, S.; Mannina, L.; Segre, A. *Tetrahedron Lett*. **2002**, *43*, 2515.
(47) Kapur, G. S.; Cabrita, E. J.; Berger, S. *Tetrahedron Lett*. **2000**, *41*, 7181.
(48) Hori, A.; Kumazawa, K.; Kusukawa, T.; Chand, D. K.; Fujita, M.; Sakamoto, S.; Yamaguchi, K. *Chem.—Eur. J*. **2001**, 7, 4142.
(49) Edward, J. T. *J. Chem. Educ*. **1970**, *47*, 261.
(50) Using the constant "6" in the Stokes—Einstein equation affords radii for small molecules that are too small. See (a) Gierer, A.; Wirtz, K. *Z. Naturforsch. A* **1953**, *8*, 522. (b) Yumet, E.; Chen, H. C.; Chen, S. H. *AIChE J*. **1985**, *31*, 76. (c) Chen, H. C.; Chen, S. H. *J. Phys. Chem*. **1984**, *88*, 5118. Equations to correct for this problem have been suggested: see ref 90a and references therein.
(51) Pregosin, P. S.; Rüegger, H. In *Comprehensive Coordination Chemistry II*; McCleverty, A., Meyer, T. J., Eds.; Elsevier: Amsterdam, 2004; Vol. 2, pp 1—36. See also ref 134 for an analogous plot for selected zirconocene salts.
(52) Martinez-Viviente, E.; Ruegger, H.; Pregosin, P. S.; Lopez-Serrano, J. *Organometallics* **2002**, *21*, 5841.
(53) Fernández, I.; Martinez-Viviente, E.; Pregosin, P. S. *Inorg. Chem.* **2004**, *43*, 4555.
(54) Nama, D.; Kumar, P. G. A.; Pregosin, P. S. *Magn. Reson. Chem.* **2005**, *43*, 246.
(55) Martinez-Viviente, E.; Pregosin, P. S.; Vial, L.; Herse, C.; Lacour, J. *Chem.—Eur. J*. **2004**, *10*, 2912.
(56) (a) Hallwass, F.; Engelsberg, M.; Simas, A. M. *J. Phys. Chem. A* **2002**, *106*, 589. (b) Hallwass, F.; Engelsberg, M.; Simas, A. M.; Barros, W. *Chem. Phys. Lett.* **2001**, *335*, 43.
(57) Pregosin, P. S.; Martinez-Viviente, E.; Kumar, P. G. A. *Dalton Trans.* **2003**, 4007.
(58) Martinez-Viviente, E.; Pregosin, P. S. *Helv. Chim. Acta* **2003**, *86*, 2364.
(59) Jerschow, N. M. *J. Magn. Reson*. **1997**, *125*, 372.
(60) Hayamizu, K.; Price, W. S. *J. Magn. Res.* **2004**, *167*, 328.
(61) (a) Hedin, N.; Yu, T. U.; Furó, I. *Langmuir* **2000**, *16*, 7548. (b) Hedin, N.; Furó, I. *J. Magn. Reson*. **1998**, *131*, 126.
(62) (a) Avram, L.; Cohen, Y. *J. Am. Chem. Soc.* **2002**, *124*, 15148—15149. (b) Mayzel, O.; Cohen, Y. *J. Chem. Soc., Chem. Commun.* **1994**, 1901.
(63) Mayzel, O.; Aleksiuk, O.; Grynszpan, F.; Biali, S. E.; Cohen, Y. *J. Chem. Soc., Chem. Commun.* **1995**, 1183.
(64) (a) Frish, L.; Vysotsky, M. O.; Matthews, S. E.; Böhmer, V.; Cohen, Y. *J. Chem. Soc., Perkin Trans.* **2002**, *2*, 8. (b) Cohen, Y.; Ayalon, A. *Angew. Chem., Int. Ed*. **1995**, *34*, 816. (c) Cohen, Y.; Avram, L.; Frish, L. *Angew. Chem., Int. Ed.* **2005**, *44*, 520. For similar systems, see: (d) Shabtai, E.; Hoffman, R. E.; Cheng, P.-C.; Bayrd, E.; Preda, D. V.; Scott, L. T.; Rabinovitz, M. *J. Chem. Soc., Perkin Trans 2* **2000**, 129.
(65) Cabrita, E. J.; Berger, S. *Magn. Reson. Chem*. **2001**, *39*, S142.
(66) Zuccaccia, C.; Stahl, N. G.; Macchioni, A.; Chen, M. C.; Roberts, J. A.; Marks, T. J. *J. Am. Chem. Soc.* **2004**, *126*, 1448.
(67) Hoefelmeyer, J. D.; Brode, D. L.; Gabbai, F. P. *Organometallics* **2001**, *20*, 5653.
(68) Pescitelli, G.; Di Bari, L.; Salvadori, P. *Organometallics* **2004**, *23*, 4223.
(69) Chen, Y.; Valentini, M.; Pregosin, P. S.; Albinati, A. *Inorg. Chim. Acta* **2002**, *327*, 4.
(70) Geldbach, T.; Pregosin, P. S.; Albinati, A.; Rominger, F. *Organometallics* **2001**, *20*, 1932.
(71) Otto, W. H.; Keefe, M. H.; Splan, J. T.; Larive, C. K. *Inorg. Chem.* **2002**, *41*, 6172.
(72) Goicoechea, J. M.; Mahon, M. F.; Whittlesey, M. K.; Kumar, P. G. A.; Pregosin, P. S. *Dalton Trans.* **2005**, *3*, 588.
(73) (a) Kronenburg, C. M. P.; Jastrzebski, J.; Lutz, M.; Spek, A. L.; van Koten, G. *Organometallics* **2003**, *22*, 2312. (b) Kronenburg, C. M. P.; Jastrzebski, J.; Boersma, J.; Lutz, M.; Spek, A. L.; van Koten, G. *J. Am. Chem. Soc.* **2002**, *124*, 11675.
(74) Knotter, D. M.; Grove, D. M.; van Maanen, H. L.; Spek, A. L.; van Koten, G. *Inorg. Chem.* **1991**, *30*, 3309.
(75) Knotter, D. M.; Grove, D. M.; Smeets, W. J. J.; Spek, A. L.; van Koten, G. *J. Am. Chem. Soc.* **1992**, *114*, 3400.
(76) Knotter, D. M.; Spek, A. L.; van Koten, G. *J. Chem. Soc., Chem. Commun.* **1989**, 1738.

(77) Pichota, A.; Pregosin, P. S.; Valentini, M.; Wörle, M.; Seebach, D. *Angew. Chem., Int. Ed.* **2000**, *112*, 153.
(78) Xie, X.; Auel, C.; Henze, W.; Gschwind, R. M. *J. Am. Chem. Soc.* **2003**, *125*, 1595.
(79) Olenyuk, B.; Lovin, M. D.; Whiteford, J. A.; Stang, P. J. *J. Am. Chem. Soc.* **1999**, *121*, 10434.
(80) Gorman, C. B.; Smith, J. C.; Hager, M. W.; Parkhurst, B. L. *J. Am. Chem. Soc.* **1999**, *121*, 9958.
(81) Valentini, M.; Pregosin, P. S.; Rüegger, H. *Organometallics* **2000**, *19*, 2551.
(82) Martinez-Viviente, E.; Pregosin, P. S. Unpublished work.
(83) Kumar, P. G. A.; Pregosin, P. S.; Vallet, M.; Bernardinelli, G.; Jazzar, R. F.; Viton, F.; Kundig, E. P. *Organometallics* **2004**, *23*, 5410.
(84) Kumar, P. G. A.; Pregosin, P. S.; Goicoechea, J. M.; Whittlesey, M. K. *Organometallics* **2003**, *22*, 2956.
(85) Alajarín, M.; Pastor, A.; Orenes, R.; Martínez-Viviente, E.; Pregosin, P. S. *Chem.—Eur. J*., in press.
(86) (a) Frish, L.; Vysotsky, M. O.; Böhmer, V.; Cohen, Y. *Org. Biol. Chem.* **2003**, *1*, 2011—2014. (b) Cohen, Y.; Avram, L.; Frish, L. *Angew. Chem., Int. Ed.* **2005**, *44*, 520.
(87) Martinez-Viviente, E.; Pregosin, P. S.; Fernandez, I. *Inorg. Chem.* **2005**, *44*, 5509.
(88) Valentini, M.; Ruegger, H.; Pregosin, P. S. *Helv. Chim. Acta* **2001**, *84*, 2833.
(89) Naidoo, K. J.; Lopis, A. S.; Westra, A. N.; Robinson, D. J.; Koch, K. R. *J. Am. Chem. Soc.* **2003**, *125*, 13330.
(90) (a) Zuccaccia, D.; Sabatini, S.; Bellachioma, G.; Cardaci, G.; Clot, E.; Macchioni, A. *Inorg. Chem.* **2003**, *42*, 5465. (b) Zuccaaccia, D.; Clot, E.; Macchioni, A. *New J. Chem.* **2005**, *29*, 430 and ref 54.
(91) Lacour, J.; Frantz, R. *Org. Biomol. Chem.* **2005**, *3*, 15.
(92) Favarger, F.; Goujon-Ginglinger, C.; Monchaud, D.; Lacour, J. *J. Org. Chem.* **2004**, *69*, 8521.
(93) Constable, E. C.; Frantz, R.; Housecroft, C. E.; Lacour, J.; Mahmood, A. *Inorg. Chem.* **2004**, *43*, 4817.
(94) For the Lacour salts shown in Table 8, we have attempted to make this approach semiquantitative; however, given all of the various assumptions made, we do not feel that our approach affords results that are better than ±5%.
(95) (a) Macchioni, A.; Romani, A.; Zuccaccia, C.; Guglielmetti, G.; Querci, C. *Organometallics* **2003**, *22*, 1526. (b) Zuccaccia, C.; Bellachioma, G.; Cardaci, G.; Macchioni, A. *Organometallics* **2000**, *19*, 4663.
(96) Fernández, I.; Martinez-Viviente, E.; Breher, F.; Pregosin, P. S. *Chem.—Eur. J.* **2005**, *11*, 1495.
(97) Metz, D. J.; Glines, A. *J. Phys. Chem.* **1967**, *71*, 1158.
(98) Kumar, P. G. A.; Pregosin, P. S.; Schmid, T. M.; Consiglio, G. *Magn. Reson. Chem.* **2004**, *42*, 795.
(99) (a) Macchioni, A. *Eur. J. Inorg. Chem.* **2003**, *2*, 195. (b) Macchioni, A. *Chem. Rev.* **2005**, *105*, 2039.
(100) Binotti, B.; Bellachioma, G.; Cardaci, G.; Macchioni, A.; Zuccaccia, C.; Foresti, E.; Sabatino, P. *Organometallics* **2002**, *21* (2), 346.
(101) Bellachioma, G.; Binotti, B.; Cardaci, G.; Carfagna, C.; Macchioni, A.; Sabatini, S.; Zuccaccia, C. *Inorg. Chim. Acta* **2002**, *330*, 44.
(102) Macchioni, A.; Zuccaccia, C.; Clot, E.; Gruet, K.; Crabtree, R. H. *Organometallics* **2001**, *20*, 2367.
(103) Macchioni, A.; Bellachioma, G.; Cardaci, G.; Travaglia, M.; Zuccaccia, C.; Milani, B.; Corso, G.; Zangrando, E.; Mestroni, G.; Carfagna, C.; Formica, M., *Organometallics* **1999**, *18*, 3061.
(104) Zuccaccia, C.; Macchioni, A.; Orabona, I.; Ruffo, F. *Organometallics* **1999**, *18*, 4367.
(105) Macchioni, A.; Bellachioma, G.; Cardaci, G.; Cruciani, G.; Foresti, E.; Sabatino, P.; Zuccaccia, C. *Organometallics* **1998**, *17*, 5549.
(106) Bellachioma, G.; Cardaci, G.; Macchioni, A.; Reichenbach, G.; Terenzi, S. *Organometallics* **1996**, *15*, 4349.
(107) Cavallo, L.; Macchioni, A.; Zuccaccia, C.; Zuccaccia, D.; Orabona, I.; Ruffo, F. *Organometallics* **2004**, *23*, 2137.
(108) Binotti, B.; Carfagna, C.; Foresti, E.; Macchioni, A.; Sabatino, P.; Zuccaccia, C.; Zuccaccia, D. *J. Organomet. Chem.* **2004**, *689*, 647.
(109) Binotti, B.; Macchioni, A.; Zuccaccia, C.; Zuccaccia, D. *Comments Inorg. Chem.* **2002**, *23*, 417.
(110) Lautens, M.; Fagnou, K. *J. Am. Chem. Soc.* **2001**, *123*, 7170.
(111) Fagnou, K.; Lautens, M. *Angew. Chem., Int. Ed.* **2002**, *41*, 27.
(112) Trost, B. M.; Bunt, R. C. *J. Am. Chem. Soc.* **1998**, *120*, 70.
(113) Evans, D. A.; Murray, J. A.; von Matt, P.; Norcross, R. D.; Miller, S. J. *Angew. Chem.* **1995**, *107*, 864.
(114) Moreau, C.; Hague, C.; Weller, A. S.; Frost, C. G. *Terahedron Lett.* **2001**, *42*, 6957.
(115) Koh, J. H.; Larsen, A. O.; Gagne, M. R., *Org. Lett.* **2001**, *3*, 1233.
(116) Kundig, E. P.; Saudan, C. M.; Bernardinelli, G. H. *Angew. Chem.* **1999**, *111*, 1297.
(117) (a) Bochmann, M. *J. Organomet. Chem.* **2004**, *689*, 3982. (b) Zhou, J.; Lancaster, S. J.; Walker D. A.; Beck, S.; Thorton-Pett, M.; Bochmann, M. *J. Am. Chem. Soc.* **2001**, *123*, 233.
(118) Schmid, T. M.; Consiglio, G. *Chem. Commun.* **2004**, 2318.

(119) Dupont, J.; de Souza, R. F.; Suarez, P. A. Z. *Chem. Rev.* **2002**, *102*, 3667.

(120) Dyson, P. J. *Appl. Organomet. Chem.* **2002**, *16*, 495.

(121) Song, C. E. *Chem. Commun.* **2004**, 1033.

(122) Attempts to use the methacrolein complex [Ru(η^5-C$_5$H$_5$)(BIPHOP−F)(CH$_2$CH(Me)CHO)][Y], met with difficulties due to the presence of small amounts of the aquo-complex [Ru(η^5-C$_5$H$_5$)-(BIPHOP−F)(H$_2$O)][Y]. The same difficulty was encountered with the indenyl complexes where [Ru(η^5-C$_9$H$_7$)(BIPHOP−F)-(H$_2$O)][Y] was present as an impurity.

(123) Tye, H. *J. Chem. Soc., Perkin Trans. 1* **2000**, 275.

(124) Ghosh, A. K.; Mathivanan, P.; Cappiello, J. *Tetrahedron: Asymmetry* **1998**, *9*, 1.

(125) Helmchen, G.; Pfaltz, A. *Acc. Chem. Res.* **2000**, *33*, 336.

(126) (a) Bartels, B.; Garcia-Yebra, C.; Helmchen, G. *Eur. J. Org. Chem.* **2003**, *68*, 1097. (b) Kollmar, M.; Steinhagen, H.; Janssen, J. P.; Goldfuss, B.; Malinovskaya, S. A.; Vazquez, J.; Rominger, F.; Helmchen, G. *Chem.—Eur. J.* **2002**, *8*, 3103. (c) Helmchen, G. *J. Organomet. Chem.* **1999**, *576*, 203.

(127) (a) Nishibayashi, Y.; Takei, I.; Uemura, S.; Hidai, M. *Organometallics* **1999**, *18*, 2291. (b) Uemura, S.; Hidai, M. *Organometallics* **1998**, *17*, 3420. (c) Nishibayashi, Y.; Segawa, K.; Takada, H.; Ohe, K.; Uemura, S. *Chem. Commun.* **1996**, 847. (d) Nishibayashi, Y.; Segawa, K.; Ohe, K.; Uemura, S. *Organometallics* **1995**, *14*, 5486.

(128) (a) Smidt, S. P.; Zimmermann, N.; Studer, M.; Pfaltz, A. *Chem.—Eur. J.* **2004**, *10*, 4685. (b) Smidt, S. P.; Menges, F.; Pfaltz, A. *Org. Lett.* **2004**, *6*, 2023. (c) Pfaltz, A.; Blankenstein, J.; Hilgraf, R.; Hormann, E.; McIntyre, S.; Menges, F.; Schonleber, M.; Smidt, S. P.; Wustenberg, B.; Zimmermann, N. *Adv. Synth. Catal.* **2003**, *345*, 33. (d) Menges, F.; Pfaltz, A. *Adv. Synth. Catal.* **2002**, *344*, 40. (e) Cozzi, P. G.; Zimmermann, N.; Hilgraf, R.; Schaffner, S.; Pfaltz, A. *Adv. Synth. Catal.* **2001**, *343*, 45054. (f) Blankenstein, J.; Pfaltz, A. *Angew. Chem., Int. Ed.* **2001**, *40*, 4445. (g) Blackmond, D. G.; Lightfoot, A.; Pfaltz, A.; Rosner, T.; Schnider, P.; Zimmermann, N. *Chirality* **2000**, *12*, 442.

(129) (a) Drago, D.; Pregosin, P. S.; Pfaltz, A. *Chem. Commun.* **2002**, 286. (b) Smidt, S. P.; Pfaltz, A.; Martinez-Viviente, E.; Pregosin, P. S.; Albinati, A. *Organometallics* **2003**, *22*, 1000. (c) Martinez-Viviente, E.; Pregosin, P. S. *Inorg. Chem.* **2003**, *42*, 2209.

(130) (a) Crabtree, R. H. *Acc. Chem. Res.* **1979**, *12*, 331. (b) Chodosh, D. F.; Crabtree, R. H.; Felkin, H.; Morris, G. E. *J. Organomet. Chem.* **1978**, *161*, C67.

(131) (a) Wang, H.; Casalnuovo, A. L.; Johnson, B. J.; Mueting, A. M.; Pignolet, L. H. *Inorg. Chem.* **1988**, *27*, 325. (b) Wang, H. H.; Pignolet, L. H. *Inorg. Chem.* **1980**, *19*, 1470.

(132) Gladysz, J. A. (Ed.) *Chem. Rev.* **2000**, *100*, 1167−1604, special issue on polymerization.

(133) Chen, M. C.; Roberts, J. A. S.; Marks, T. J. *J. Am. Chem. Soc.* **2004**, *126*, 4605 and references therein.

(134) (a) Babushkin, D. E.; Brintzinger, H. *J. Am. Chem. Soc.* **2002**, *124*, 12869. (b) Beck, S.; Geyer, A.; Brintzinger, H. H. *Chem. Commun.* **1999**, 2477.

(135) Stahl, N. G.; Zuccaccia, C.; Jensen, T. R.; Marks, T. J. *J Am. Chem Soc.* **2003**, *125*, 5256.